It's Our Fault – Synthetic Seismicity of the Wellington Region: Final Report

Russell Robinson
Nicola Litchfield
Russ Van Dissen

GNS Science Consultancy Report 2009/192.
July 2009

GNS SCIENCE
TE PŪ AO

DISCLAIMER

BIBLIOGRAPHIC REFERENCE

Robinson, R.; Van Dissen, R.; Litchfield, N.; 2009. It's Our Fault – Synthetic Seismicity of the Wellington Region: Final Report, *GNS Science Consultancy Report* 2009/192. 40 p.

CONTENTS

EXECUTIVE SUMMARY ..... **III**

1.0 AIM **1**

2.0 SYNTHETIC SEISMICITY **1**

3.0 GENERAL ASPECTS OF WELLINGTON SEISMICITY **3**

4.0 THE WELLINGTON FAULT NETWORK **4**

5.0 THE "STANDARD MODEL" AND ITS TUNING **6**

5.1 Slip Rates 6
5.2 b-value 6
5.3 Rate of Activity 7
5.4 Spatial Distribution of Background Activity 7
5.5 Area – Moment Scaling 7

6.0 EMERGENT FEATURES OF THE STANDARD MODEL SEISMICITY **8**

6.1 Regional Moment Release 8
6.2 Recurrence Time Statistics 8
6.3 Regional Recurrence Time and Fault Interaction Matrix 8

7.0 THE WELLINGTON-HUTT VALLEY SECTION OF THE WELLINGTON FAULT **9**

8.0 SENSITIVITY TESTS **11**

9.0 CONCLUSIONS **11**

REFERENCES **12**

TABLES

Table 1 Fault and Segment Data 16
Table 2 Mechanical Properties of the Standard Model. 18
Table 3 Emergent Fault Properties 18
Table 4 Results of Sensitivity Tests. 19

FIGURES

Figure 1 Map of the Wellington Region and the major faults above the plate interface. The numbers correspond to those in Table 1 except that a few are left out due to over-crowding. The Wellington-Hutt Valley section of the Wellington Fault is highlighted in red. The coordinate system is taken from the New Zealand Map Grid with the centre redefined as the position of the WEL seismograph station at Kelburn. 20

Figure 2 Map of the Wellington Region showing the surface projections of the section of the plate interface on which seismic slip is allowed (red). The yellow circles represent the 1000 small, random faults above the plate interface. The green circles represent the 2000 small, random faults below the plate interface. 21

Figure 3a Comparisons of the long-term slip rates for the synthetic model and those observed geologically (in mm/year). **A**: for the strike-slip component (negative if right-lateral). **B**: For the dip-slip component (negative is for normal faulting, positive for thrust). Circles are for the subduction interface. 22

Figure 3b Comparisons of the long-term slip rates for the synthetic model and those observed geologically (in mm/year). **A**: for the strike-slip component (negative if right-lateral). **B**: For the dip-slip component (negative is for normal faulting, positive for thrust). Circles are for the subduction interface. 23

Figure 4 Frequency – Magnitude plot for the region as a whole. Note that the numbers are not cumulative. 24

Figure 5 Frequency – Magnitude plots for two individual faults that show extreme types of behaviour. **A**: Gutenberg-Richter behaviour for the Alfredton-Makuri Fault. **B**: Characteristic behaviour for the Kekerengu Fault. 25

Figure 6 Example of the spatial distribution of hypocentres in the synthetic catalogue for the time period 55,000 -56,000 years. **Top**: Map view of all epicentres. **Bottom**: NorthWest – SouthEast cross-section. 26
Figure 7 Moment scaling for characteristic events. Horizontal axis = log10(Moment) expected from the scaling relations of Webb et al. (1999). Vertical axis = Moment of characteristic events form the synthetic seimicity model. Red dot = Whaekaukau Fault. Red dashed line shows a ration of 1:1. 27
Figure 8 Cumulative moment release vs. time for the period 55,000 – 56,000 years. Note the considerable variations over time spans of 100 – 200 years which would make extrapolating the actual historic record very dangerous. 28
Figure 9 Distribution of recurrence time for characteristic events on any fault. The red curve is for the synthetic catalogue, the green for a randomized catalogue. Events in the synthetic catalogue show considerable short-term temporal clustering followed by relative quiescence. 29
Figure 10 Interaction matrix for characteristic events. A circle is plotted if the number of events on Fault 2, within 10 years following a n event on Fault 1, is significantly larger than expected by chance. Large red circles = bigger by a factor of 15 or more; orange circles = bigger by a factor of 10 - 15; yellow circles = bigger by a factor of 5 - 10; green if bigger by a factor of 2.5 – 5.0. Numbers on the axes refer to the fault number as in Table 1 and Figure 1. Note that the Wellington – Hutt Valley Fault (7) is not often triggered by any other fault. 30
Figure 11 Frequency – Magnitude plot for the Wellington-Hutt Valley section of the Wellington Fault. The vertical black line shows the definition of M_{char}. 31
Figure 12 Histogram of recurrence time for characteristic events on the Wellington-Hutt Valley section of the Wellington Fault. The black line and symbols shows the best fitting 3-parameter Weibull distribution. 32
Figure 13 Moving average recurrence time vs. time for the characteristic events on the Wellington-Hutt Valley section of the Wellington Fault. Top: Averaged over four instances (5 events). Bottom: Averaged over 10 instances (9 events). Note that the vertical scales are different. 33
Figure 14 Cartoon showing how the two classes of recurrence time on the Wellington-Hutt Valley section of the Wellington Fault are different. 34
Figure 15 Normalized histograms for the two classes of recurrence times for characteristic events (M 7.35 or more) on the Wellington-Hutt Valley section of the Wellington Fault. Note that for each 100 year bin there are two bars, one red, and one green, for the same bin but displaced for clarity. 34
Figure 16 Normalized histograms for the two classes of recurrence times for moderate events (M 6.5 – 7.3) on the Wellington-Hutt Valley section of the Wellington Fault. 35
Figure 17 Histogram for the positions of epicentres of characteristic events on the Wellington-Hutt Valley section of the Wellington Fault. The horizontal axis is the distance along the fault measured from the south end. 36

EXECUTIVE SUMMARY

A computer synthetic seismicity program for the Wellington region has been implemented and used to infer the effect of the 1848 Awatere and 1855 Wairarapa mega-earthquakes on the timing of the next characteristic (magnitude 7.35 or more) earthquake on the Wellington-Hutt Valley section of the Wellington Fault. We find that, on average over several hundred cases, a Wellington Fault event is delayed by 259 years. The synthetic catalogue of 500,000 events, magnitude 5.5 or more, also gives the average recurrence time of characteristic Wellington Fault events (960 years) and their Coefficient of Variation (0.40). There is also a strong retarding effect on moderate magnitude Wellington Fault events, magnitude 6.5 – 7.3. Sensitivity tests indicate that these results are robust. The synthetic model contains 58 known major faults and 3000 randomly placed small faults in order to reproduce the rate and spatial distribution of background seismicity observed recently. From the synthetic catalogue it is possible to determine the average recurrence rate for all major faults. Also, there is strong evidence of the short-term (10 years) temporal clustering of large events throughout the region, a factor that contributes to a highly variable moment release rate over time spans of a few hundred years.

1.0 AIM

The primary aim of the synthetic seismicity aspect of It's Our Fault is to evaluate how the occurrence of recent large earthquakes in the region (1848, Awatere Fault, magnitude 7.8; 1855, Wairarapa Fault, magnitude 8+) have influenced the timing of large events on the Wellington-Hutt Valley section of the Wellington Fault. Also, how might the subduction interface under the region affect the situation? Simple induced stress models for the Wairarapa-Wellington fault interaction indicate that the 1855 event would have de-stressed much of the Wellington-Hutt Valley section of the Wellington Fault (Han, 2003). But experience with models of other complex fault networks has shown that this can be misleading as the many fault interactions, complex slip distributions and dynamic rupture propagation destroy any such simple relation. Certainly simple one-on-one models using planar faults with uniform slip in pre-specified events cannot be used for quantitative studies. A full synthetic seismicity model incorporating all the major (and many minor) faults of the greater Wellington region, spanning a long time period, is needed for reliable statistical estimates of how the Wellington Fault hazard may change in time. Such a synthetic model can also address many other important questions regarding the seismicity of the region, such as recurrence times (and their variability) and event clustering or shadowing. A secondary aim of the synthetic seismicity study is to generate detailed examples of slip on the Wellington Fault that can be used to calculate strong-ground motion at various sites. This aspect is not treated in this report since much of that work is part of a separate study.

2.0 SYNTHETIC SEISMICITY

An often lamented fact is that the instrumental, historic, and paleoseismic records of past earthquakes in New Zealand are too short, too incomplete, too inhomogeneous or too uncertain to enable us to answer some basic questions to do with seismic hazard. In the greater Wellington region, for example, reasonable instrumental records extend back only to about 1940. Historic records extend back to only about 1840. Paleoseismic results are still very incomplete and the dates of past large quakes are often highly uncertain. Thus we cannot reliably answer questions concerning the frequency of large events in the region, on what faults they occur, and how often they may occur in temporal and/or spatial clusters.

In recent years the field of study termed "synthetic seismicity" has developed in order to help address these problems (Dieterich, 1994; Ben-Zion, 1996; Robinson & Benites, 1996; Ward. 2000; Fitzenz & Miller, 2001; Rundle et al., 2006; Robinson, 2004; Robinson et al, 2009). By synthetic seismicity we mean a computer model of a fault network that generates catalogues of earthquakes based on our knowledge of the physics of seismogenesis and fault interaction. Such catalogues are, by definition, homogeneous (e.g., magnitudes are calculated uniformly through time), can be as long as our patience and computer resources allow, and are complete to the degree that all the known major faults are included along with many more smaller ones. The models are "tuned" to reproduce observed data on real seismicity (e.g., b-value, rates of activity) and geologic data on the long-term slip rates, known or estimated. Generally the catalogues are made long enough to yield statistically reliable information and to sample the complete range of interactions amongst events. We can then use the catalogues to answer questions about large event recurrence times and their temporal variations, either for a single specific fault or for the region as a whole. The possibility of event triggering, clustering or shadows, can also be examined.

Of course, the answers to our questions are believable only if the synthetic model captures real-world fault behaviour to an acceptable degree. The synthetic seismicity model used in this study is very similar to that described fully by Robinson & Benites (1996, 2001), Robinson (2004) and Robinson et al. (2009). The model differs from most others in that faults of any orientation and sense of slip are embedded in a fully 3D elastic half-space, fault rupture is pseudo-dynamic, the cell size (each fault is sub-divided into smaller cells) can be small enough that rupture histories can be used to generate strong-motion seismograms, and induced changes in pore pressure are included. Except for the pore pressure aspects, the model as used here is entirely elastic, but visco-elastic relaxation is approximated in some runs as part of a sensitivity analysis.

The model consists of five key elements: 1) A geometric description of the faults, which are finely divided into smaller cells (2.5 x 2.5 km here); 2) frictional behaviour defined by a variable coefficient of friction and of static/dynamic type, with healing; 3) a driving mechanism that loads the faults toward failure; 4) fault failure based on the Coulomb Failure Criterion; and 5) fault interactions via induced changes in static stress and pore pressure. The driving mechanism results in the initial failure of one fault cell that in turn induces changes in stress/pore pressure on all other cells, on all faults, after allowing for stress propagation time. If loaded sufficiently, other cells then fail as part of the same event, and so on. The more cells that slip during a failure episode the bigger is the synthetic earthquake. Thus, once the initial conditions of the model have been specified, the model is deterministic, not stochastic. The formulation of Okada (1992) for a uniform elastic half-space is used to calculate the induced displacements and their spatial derivatives, and hence strains and stresses. Induced stresses propagate through the medium at the shear-wave velocity. The model rigidity is 4.0 x 10^{10} Nm^{-2} and the density is 2.65 x 10^{3} kgm^{-3}. These average values are considered to be reasonable first approximations for the brittle crust in New Zealand. The coefficients of friction (dry, and variable from cell to cell) range from 0.7 to 0.8 in our preferred model, but other ranges are also investigated. We do not use the more common “apparent coefficient of friction” that only approximates the effect of pore pressure, because we prefer the more realistic treatment in which pore pressure changes can be positive or negative, in proportion to the induced dilation or compaction (Beeler et al., 2000) and decay with time. This does involve the assumption of a constant Skempton’s coefficient, here taken as 0.5. The stress drop on a cell that fails is uniformly 30%, and healing occurs after 3.0 seconds (Heaton, 1990).

An important additional factor in our program is what we call the “dynamic enhancement factor”, DEF). This factor gives the amplification of the induced stresses near the edges of a propagating rupture front. It is applied only for one (very short) time step and only for the immediate neighbours of a rupturing cell (Robinson & Benites, 2001). The DEF is meant to mimic the stress enhancements found in more detailed models of crack propagation that would require much too much computation in our case. It has two primary effects: 1) ruptures tend to cascade more easily; and 2) ruptures can sometimes jump across from one fault segment to another offset segment if the two segments are not too far apart. The value used here, 3.0, was not picked arbitrarily, but is that value found necessary in our previous work to match detailed computational studies of en echelon faults (Harris & Day, 1999) and to match the probability of jumps as observed in the real world, i.e. about 50% for a separation of 1 km. (Wesnousky, 2008).

Because the synthetic seismicity program is computationally intense, the success of the project depends on calculating all cell interaction terms at the start and storing them in memory. This in turn places a limit of the extent of the fault network and the cell size. Another aspect that decreases computation is that there are two sizes of time step. The first is quite short (0.8 sec here, based on cell size and stress propagation velocity) and is used during the rupture process and the second is variable and much longer, corresponding to the time needed for the next rupture episode to start (this can be calculated from the loading rates and current stresses). For this project, most computations have been done on GNS Science's parallel processing computers.

Our synthetic seismicity program, sometimes known as ARTS (ARTifical Seismicity), was first applied to a study of the Wellington region in 1996 (Robinson & Benites, 1996). That was a study that involved only the 6 most major faults and was designed to answer EQC's concern about multiple large events within a short time span. The answer was that close temporal clustering of large events was likely. Also there was a lot of interaction between subduction interface earthquakes and the Wairarapa Fault. Since then the program, or its extensions (Robinson, & Benites, 2001), have been used to study the Marlborough fault network (Robinson, 2004) and the Taupo rift (Robinson et al., 2009). The program has also been presented to a SCEC (Southern California Earthquake Consortium) workshop. Another study focused on the Wellington Fault in isolation (as a single planar segment) for producing detailed time histories of a characteristic rupture and the calculation of the corresponding strong ground motion (R. Benites, personal communication).

3.0 GENERAL ASPECTS OF WELLINGTON SEISMICITY

Since the deployment of relatively closely spaced seismographs in the Wellington region (Figure 1) in about 1978 (and progressively onwards) it has become known that the majority of day-to-day background seismicity occurs within the subducted Pacific Plate, primarily below about 20 km depth (Robinson, 1986; Reyners & Eberhart-Phillips, 2009). These events have almost exclusively normal mechanisms, generally attributed to down-dip directed "slab pull" being resisted by a locked plate interface. Or they may be due to slab bending. They increase markedly in number NW of a line along the Wairarapa depression (a "seismic front"). These events can range in magnitude up to 6.0 (as near Cape Campbell, 1977) or even 7.0 as in the second 1942 Masterton quake (Downes et al.., 2001; Webb & Anderson, 1998). Some of them of small to moderate size have been clearly triggered by aseismic slip on the subduction interface further down-dip (Reyners & Bannister, 2007).

Above the plate interface, the smaller events today mostly reflect a mix of strike-slip and thrust faulting, generally in accord with plate convergence in an east-west direction. At the present day, there is very little, if any, activity clearly associated with thrusting on the plate interface itself.

Since 1986, the rate of activity for events in the Wellington region of magnitude 4.0 or more is 19 events/year. The b-value (slope of the frequency-magnitude plot) is close to 1.0.

In the greater Wellington region large, shallow (above the plate interface) earthquakes occur in the historical record, including magnitude 7.8 on the Awatere Fault in 1848 (Grapes et al., 1998), magnitude >8.0 on the Wairarapa Fault in 1855 (Grapes & Downes, 1997; Darby & Beanland, 1992), magnitude 7.4 on the Alfredton-Makuri Fault in 1934 (Downes et al., 1999) and magnitude 7.2 near Masterton in 1942 (Downes et al., 2006). Schermer et al. (2000)

suggest that the 1934 quake occurred on the Waipukaka Fault. The causative fault for the 1942 event is considered here to be the Carterton Fault, but the field evidence is unclear. There is paleoseismic and ocean bottom survey evidence for pre-historic large events on the Wairau (Grapes & Wellman, 1986; Zachariasen et al. 2006), Ohariu (Litchfield et al., 2004), and at least three off-shore faults (Barnes & Audru, 1999; Pondard et al., 2007; Barnes et al. 2008).

The occurrence, or not, of large subduction interface thrust events under Wellington is unclear. GPS results (Wallace et al. 2004; Beavan and Wallace, 2008) indicate strongly that strain is accumulating on at least some parts of the interface. North-east of Cook Strait there appears not to be enough arc-normal convergence on shallow faults to account for the full plate tectonic convergence rate (Nicol & Beavan, 2003; Nicol et al., 2007). South-west of Cook Strait structures such as the Jordon Thrust and offshore faults can probably account for enough convergence so that little slip on the underlying subduction interface is needed. There is a possibility that NE of Cook Strait the convergence is taken up primarily by aseismic slip on the plate interface. Aseismic slip episodes are regularly detected in the Wellington region via continuous GPS observations with equivalent magnitudes of up to 6.5 (Wallace et al., 2009). And there is little or no evidence for the widespread coastal uplift that would be expected to accompany a large (seismic) thrust event on the interface (K. Berryman, personal communication, 2008). It is important to note that as far as static stress interactions are concerned, the effects of seismic vs. aseismic slip are much the same. The Wairarapa Fault, source of the massive 1855 quake, is generally thought to be listric (Darby & Beanland, 1992), the north-westward dip decreasing as the fault approaches the plate interface. Surface deformations due to the 1855 event are not well enough known to unambiguously know if slip in that event extended down onto the plate interface. If it did, then perhaps this combined with aseismic slip and offshore thrust faulting is sufficient to account for the convergence. Just to the north of the Wellington region Nicol & Beavan (2003) estimate that ~80% of the arc-normal convergence is taken up on the subduction interface.

4.0 THE WELLINGTON FAULT NETWORK

The fault network in this study consists of two types of fault. First there are 55 major faults above the plate interface that reach the surface (Figure 1, Table 1), plus three sections along the plate interface where GPS data indicate elastic strain is accumulating (Figure 2, Table 1, faults 56-58). Second there are 3000 smaller faults distributed randomly throughout the region except that the fault density approximates the distribution of real, recent seismicity; these small faults are not meant to correlate with any particular geologic feature.

The choice of major faults was based on geologic mapping (GNS Science Active Fault Database, http://data.gns.cri.nz/af) and marine sea floor mapping (Barnes et al., 2008; P. Barnes, personal communication, 2009). It is thought that most faults in the greater Wellington region (Figure 1) that reach the surface and are capable of generating an event of magnitude 6.5 are included. Note, however, that the “region” does not extend as far as the Waimea Fault north-east of Nelson. Each major fault was approximated by 1 to 5 planar segments of constant strike and dip. The strikes are well constrained but in some cases the dip is uncertain (this is the case for the Wellington Fault in particular). Slip directions and long-term rates of slip (considering fault segments separately) are based on in-house discussions at GNS Science (R. Van Dissen, N. Litchfield, R. Langridge, K. Berryman and M. Stirling, personal communications, 2008). The adopted values are all listed in Table 1. Since

there are many dipping faults it sometimes happened that faults intersected at depth. In that case, the fault with the lesser slip rate was cut-off.

The locations of regions on the plate interface that are included are shown in Figure 2. The choice is based on recent GPS inversion studies (similar to Wallace et al., 2004). Note that the north-east section consists of two "segments" due to the increase in dip on the interface to the north-west.

The loading mechanism in this study consists of simple increments in shear stress on each major fault segment. The initial trial used stress increments in proportion to the long-term geologic slip rate and direction. The synthetic seismicity catalogue that resulted showed that the model long-term slip rates were sometimes quite different from the geologic ones. The highly non-linear nature of the synthetic seismicity model means that you cannot simple increase or decrease each segments loading rate in proportion to the error. This leads to the use of a number of trial-and-error adjustments until the model and observed rates are close, considering the possible errors in the former. The case is somewhat different for the plate interface where the shear stress loading for shallower parts was in the plate tectonic convergence direction whereas it was down-dip in the deeper sections, reflecting the likely decoupling between the subducting and over-riding plate at depths greater than about 40 km.

It would be desirable to have a loading mechanism that is more in line with ideas of plate convergence, i.e. compression in an east-west direction acting on the edges of the model. However, such a loading mechanism is inconsistent with the rapid changes in fault slip rate on neighbouring faults. In the end, our loading mechanism is just a convenient way to mimic the real loading process, whose mechanism we don't fully understand.

In addition to the major faults, there were 3000 smaller faults placed at locations so as to better simulate the distributed of recent background seismicity (Figure 2). The small faults also tend to relieve the induced normal stresses produced by the major dipping faults on themselves that might otherwise accumulate over long times (making them unrealistically weak or strong). Although our model is not a continuum model, the small faults help to approximate that for very much less computation than, say, a finite element model would require.

The greater part (2/3) of the small, random, faults were placed within the subducted Pacific plate lithosphere and were taken as normal faults that could dip either 60 degrees north-west or south-east, striking more-or-less parallel to the margin (~45^{o}). The biggest could be the source of an event as big as the second (deeper) 1942 Wairarapa quake (magnitude 7.0). The remainder of the small faults were placed at random spots above the plate interface, with strikes and dips perturbed slightly from those of the nearest major fault. The loading rate of the small faults below the plate interface was taken as larger than that for those above, to better match today's observed relative rates of activity. The same effect could be achieved with just much larger numbers of faults below the interface, but this leads to a number of cells that is too large for efficient computation. The loading mechanism for the small faults below the plate interface was simple accumulation of shear stress in the down-dip direction. Above the plate interface, there was accumulation of shear stresses in a direction close to that of the nearest major fault.

5.0 THE "STANDARD MODEL" AND ITS TUNING

"If it looks like a duck, swims like a duck and quacks like a duck, then it probably is a duck."

James W. Riley, 1849 – 1916.

Except when we come to the subject of sensitivity tests, the synthetic seismicity results we will discuss are based on a "Standard Model" using the fault network as described above and our preferred mechanical properties. The mechanical properties (and their range of variation) are the same for all faults in the model and are listed in Table 2. Seismic slip on the plate interface is also included. Our preferred values come from extensive previous studies (published and not published) and examination of the relevant literature.

The Standard Model catalogue includes 500,000 events, magnitude 5.10 – 8.29, over a time span of about 520,000 years. At the beginning of a model run the coefficients of friction (different for each cell) are picked at random from within the specified range (0.7 – 0.8). The initial stress on each cell is also a random percent of the failure level. Because these initial values, together with the fixed parameters and network geometry, do not produce a mechanically stable stress configuration, it takes about 50,000 years of model time to come to equilibrium. This process is monitored by plotting the b-value vs. time, the value starting out way too low. All results discussed here omit the first 50,000 years of the catalogue.

The process of "tuning" the synthetic model involves getting it to reproduce: 1) the long-term geologic slip rates; 2) the regional b-value (slope of the frequency vs. magnitude graph) close to -1.0; 3) the regional rate of activity; 4) the spatial distribution of background activity; and 5) the Area (or Length) vs. Moment scaling as observed in New Zealand.

5.1 Slip Rates

Because on the highly non-linear nature of the model, the initial guess at loading rates does not yield long-term slip rates in very good accord with the observed slip rates. But simply adjusting the loading rate up or down on one fault segment has repercussions on all the other segments. So it is necessary to adopt a trial-and-error adjustment procedure, adjusting one or several loading rates and then re-running the model. For the Standard Model ten attempts were required to get satisfactory results. As each model test run takes about 5 days (for 250,000 events) on the GNS parallel computer "Evison", this is one of the more time-consuming aspects of a synthetic seismicity study. Even so, the match of observed and model long-term slip rates is not perfect (Figure 3), but we think it is good enough given the likely uncertainties in the observed rates which are typically +/- 20-40 % (A. Nicol, personal communication, 2009).

5.2 b-value

The b-value for the entire Standard Model catalogue is about 1 (Figure 4) with a "characteristic" hump at larger magnitudes (note that the figure shows the non-cumulative numbers as we think that is more honest than using cumulative numbers). The b-values for individual faults are variable in nature, some showing a Gutenberg-Richeter (G-R) type of distribution (Figure 5a) and others showing a clear "characteristic" type of behaviour (Figure 5b). Generally, faults near the centre of the model tend toward a G-R distribution, perhaps because they suffer more strong interactions with other faults. There is also a tendency for

higher slip rate faults to behave in a characteristic way, “doing their own thing”. The Kekerengu Fault for example, has the highest slip rate and is near the model edge, and shows a clear characteristic behaviour.

5.3 Rate of Activity

When comparing the overall rate of activity in the synthetic catalogue to that observed in the real world we encounter the problem of the plate interface. Since 1978, hypocentres in the Wellington region have become accurate enough to distinguish events likely to be on the plate interface from those above and below. There have been no events since 1978 on the interface with magnitude greater than 5.1, the lowest magnitude in the synthetic catalogue. Yet if we allow the interface in the synthetic model to behave as any other fault, there are many. The simplest explanation is that slip on the plate interface occurs aseismically, either as slow slip events as observed by GPS or as steady creep. If that is the case, the numbers we need to compare are: 1) events in the synthetic catalogue with magnitudes 5.1 or more, excluding those on the plate interface, for periods of 31 years, and 2) the instrumental record of real seismicity, magnitude 5.1 or more 1978-2008. The second number is ~43. The first number is highly variable, from 11 to 68, average 32.9 or ~ 1/year. If the plate interface events in the synthetic model are included in the count, the second number ranges from 20 to 83, average 45.4. Given the variability of the synthetic catalogue’s number, the match to the observed number is acceptable regardless of the plate interface events.

5.4 Spatial Distribution of Background Activity

The spatial distribution of synthetic seismicity above the plate interface, for periods of 31 years, varies considerably, so it makes it difficult to compare it to what has actually been observed in the real 31 years, 1978-2008. However, Figure 6 shows the synthetic events for a 1000 year period (55,000 – 56,000 yrs) in map view and as a NW-SE cross-section. The event spatial distribution looks similar to the real case, especially in cross-section (Robinson, 1986).

5.5 Area – Moment Scaling

Characteristic magnitudes, M_{char}, have been determined for all 57 major faults (Table 3). These are based on visual examination of the individual fault frequency-magnitude plots or, if that is not sufficient, on the criterion that a characteristic event ruptures 80% or more of the fault area. These have been converted to moment Mo (Nt-m) using the relation (Aki & Richards, 2002):

$$Log_{10}(Mo) = 1.5 * M_{char} + 9.045 \quad (1)$$

Figure 7 shows a plot of $Log_{10}(Mo)$ for the synthetic model characteristic events vs. that calculated from the faults’ length, L km, and width, W km, using the regression of Webb et al. (1999) which is based on New Zealand data for low to moderate slip rate faults:

$$Log_{10}(Mo) = 15.33 + log_{10}(W) + 2 * log_{10}(L) \quad (2)$$

While there is considerable scatter we think the correspondence is satisfactory. There seems to be a tendency for the larger faults to produce characteristic events somewhat smaller than would be predicted from the L and W (this is more in line with overseas data). The Wharekauhau Fault, a thrust branching off the southern Wairarapa Fault has an anomalously

low M_{char}. Other thrust faults are better behaved. So this is not likely to be a bias problem for thrust faults as opposed to strike-slip faults.

Considering the above results we feel that the standard synthetic seismicity model produces realistic synthetic events and synthetic seismicity.

6.0 EMERGENT FEATURES OF THE STANDARD MODEL SEISMICITY

6.1 Regional Moment Release

Figure 8 shows the cumulative moment release vs. time for the entire Wellington region, for all faults and all magnitudes, for 1000 years. The very long-term rate is, of course, determined by the fault loading rates. But the rate on time scales of 100 – 200 years is very uneven. This makes it difficult to argue that the present quiescence (since 1942) is a good indication of the future. The figure shows that there are periods of that length with very different behaviours.

6.2 Recurrence Time Statistics

Once the characteristic magnitudes for events on each major fault are identified we can extract information about the time between such events, for each fault separately. These "recurrence times" are an important input to seismic hazard models. Also important are the Coefficients of Variation (CVs) given by the standard deviation of the recurrence times divided by the mean. A CV close to 1.0 indicates random behaviour, a value less then1 indicates some quasi-periodic behaviour, while some clustering is indicated by values greater than 1.0. The average recurrence time and its CV for each major fault is shown in Table 3. The CV ranges from 0.1 (Vernon Fault) to 0.98 (Otaki Forks Fault) with an average of 0.51.

Some entries in Table 3 may seem odd (e.g., very long recurrence time) but this is usually because the fault in question does not have a well defined class of characteristic events. Some care should be taken if using those results for other purposes.

6.3 Regional Recurrence Time and Fault Interaction Matrix

A basic premise of the synthetic seismicity model is that faults interact via slip induced changes in Coulomb Failure Stress (dCFS; Harris, 1998):

$$dCFS = dShear + \mu * (dNormal - dPP) \quad (3)$$

where dShear is the induced change in shear stress, μ is the coefficient of friction, dNormal is the induced change in normal stress, and dPP is the induced change in pore pressure. dPP is given by:

$$dPP = K * (d\tau_{11} + d\tau_{22} + d\tau_{33}) \quad (4)$$

where K is Skempton's Coefficient (-0.5 here, see Beeler et al., 2000) and τ is the stress tensor. All model cell slips induce dCFS on all other cells after an appropriate time delay. Examples of fault interaction in the real world abound (for reviews see Harris (1998) and King & Cocco (2000)).

One way to examine interactions in the Standard Model is to first extract a list of

characteristic events (i.e., events with M >= M_{char} for the fault involved) and then examine the distribution of times between successive events, taking all faults together. This distribution can be compared to that expected for random occurrence times. This is shown in Figure 9. It can be seen, in the synthetic model, that following a characteristic event (on any fault) there is an enhanced number of cases where the next characteristic event (on any fault) occurs within 5-10 years, compared to a random event distribution. Beyond that recurrence time, the number of cases is less than random, out to about 65 years. In simple words, if we have a big event in the Wellington region there is an immediate risk of further big events, but after 10 or so years you can rest a bit easier for a while. Note from the figure that the average time between characteristic events is 40 years, although there are rare occurrences of much longer recurrence times, > 150 years with a maximum of 415 years. In the Wellington region there have been five events that could be classed as characteristic (four recurrence times) since 1840. Events in 1848, 1855, 1934, 1942, and 1942 give recurrence times of 7, 79, 8 and 0 years, an average recurrence time of 23.5 years. If we count the elapsed time since 1942 (68 years) then the average goes up to 32 years. Actually the second 1942 Masterton event, below the plate interface, occurred on a fault with no explicit analogue in the synthetic model and hence could be excluded, for an average recurrence time of 41 years! The 1848-1855 and 1942-1942 event pairs are good examples of short-term clustering.

The data shown in Figure 9 and discussed above do not identify the faults that most tend to interact with which other. This can be examined by use of an “interaction matrix” (Figure 10). In the figure fault pairs are denoted by a circle when the number of characteristic events on fault 2 (Y-axis) that follow within 10 years a characteristic event on fault 1 (X-axis) exceeds the number expected using random event times by factors of 15 (large red), 10 (medium size orange), 5 (medium size yellow) or 2.5 (small green). The green cases are sometimes not significant, but the large red ones are very unlikely to be due to chance. Since the fault numbers are assigned in order of slip rate (except the subduction interface, 56-57), the data in the figure show that it is relatively rare for a slow moving fault to trigger activity on a faster moving fault. The strongest interactions are the Booboo Fault (6) triggering both the Campbell Fault (17) and the subduction thrust. The Cloudy Bay Fault (25), in Cook Strait, seems to be triggered quite often by other, larger, nearby faults. In contrast to the earlier work of Robinson & Benites (1996) the subduction thrust events don’t seem to trigger activity elsewhere. The major causes of this difference are that in the present model the faults are much finer grained and also the seismic area on the interface is much smaller (based on GPS results not available in 1996). It is rare for the largest subduction events to cover most of even this smaller area.

7.0 THE WELLINGTON-HUTT VALLEY SECTION OF THE WELLINGTON FAULT

The Wellington-Hutt Valley section of the Wellington Fault (WF), the prime target of this study, extends from 20 km off the south coast, through Wellington City, along the western side of the harbour and Hutt Valley to Te Marua (Figure 1; shown in red). In our model it is composed of five segments.

Figure 11 shows the frequency-magnitude graph for events on the WF, from which the characteristic magnitude is determined as 7.35. This is the magnitude beyond which the number of events jumps up from an extrapolation of lower magnitude numbers. The average horizontal slip in the characteristic events is 7.1 m. The cell size of 2.5 km means it is not

possible to infer exact values of the slip for the ground surface. The standard deviation of the average slip is 0.75 m meaning it is quite possible for the average slip over a series of four or five events to vary a lot. The real-world observed average slip for four or five events is 5.0 +/- 1.3 m (Little et al. in preparation) but the site is near the northern end of the fault where we expect the slip to be less than the overall average.

The average recurrence time of characteristic events on the WF is 960 years, with a CV of 0.40. This is in good accord with recent paleoseismic estimates for the last five events (R. Van Dissen, personal communication, 2009; Langridge et al., 2009). Figure 12 shows the distribution of the recurrence times and the best fitting 3-parameter Weibull distribution. Two things to note are: 1) the lack of short (<500 years) recurrence times; and 2) the occurrence (albeit rare) of very long (>2000 years). By using the 3-parameter Weibull distribution rather than the more common 2-parameter version, the lack of short recurrence times can be well fit. However, none of the commonly used statistical distributions (e.g., Weibull, log-normal, Brownian passage time) can match the very long tail (very long recurrence times). We prefer the Weibull distribution because it has the property of an event's occurrence probability increasing monotonically with time until it does occur (Abaimov et al., 2008).

Figure 13 shows the recurrence time vs. time when averaged over 4,and 8 instances. It can be seen that there is reduced but still significant variability even at the longest averaging span. This implies, for example, that a small sample of events taken from a paleoseismic study (e.g., trenching or terrace offsets) may not be a very precise predictor of future behaviour.

It is always tempting to try to predict the next recurrence time from the previous ones. It is sometimes assumed that a long recurrence interval will be "balanced" by a short one next, and vice versa. However, the series of WF recurrence times shows very little predictability. Even a neural-network cannot predict the next recurrence time from the previous five any better than simply taking the average. (A neural-network is a non-parametric statistical learning procedure that is very good at detecting and modelling complex non-linear relations in a time series, see Reed & Marks; 1999)

The specific question this report addresses is how the occurrence of the 1848 and 1855 mega-earthquakes might affect the timing of the next characteristic event on the WF. We address this question by comparing two histograms of WF recurrence times, one for the recurrence times that include an embedded 1848/1855 event pair, and one for recurrence times that do not . The idea is illustrated schematically in Figure 14. We find that the average recurrence time when encompassing an 1848/1855 pair is 1149 years and 890 years when not, a difference of 259 years (Figure 15). In other words, the occurrence of an 1848/1855 pair retards the next WF event by 259 years, on average. We also find that very long WF recurrence times, 2000 years or more, occur only when an 1848/1855 event pair is embedded.

We have also examined the effect of 1848/1855 event pairs on the occurrence of moderate magnitude (6.5-7.3) events on the WF. For these events the retardation is, if anything, stronger (Figure 16).

We have also looked at the distribution of hypocentres of characteristic events on the WF. The hypocentre marks the point where the event initiated, and ruptures would extend outward from there. We find that very few events initiate on the southern half of the fault

(Figure 17). Most characteristic events either rupture bilaterally from near the centre or propagate to the south-west after initiating on the north-east section of the fault.

8.0 SENSITIVITY TESTS

In order to get an idea of how robust the above results are, we have compared the results for models in which we changed some parameter. The model outputs that we compare are the average WF recurrence time and its CV, and the recurrence time bias caused by an 1848/1855 event pair. The parameters varied include the WF dip, the average WF coefficient of friction, the presence or not of slip on the plate interface, the base level of pore pressure, the presence or not of a large asperity on the WF, the healing time in the fault friction law, the presence or not of the numerous small faults, the presence or not of viscoelastic relaxation (approximated only), the percent stress drop on cell failure, and several values of the dynamic enhancement factor. As described above, the synthetic seismicity model involves assigning each cell a coefficient of friction randomly within a specified range. We have also examined the outputs for models when the randomization is done with different "seed" values.

Table 4 lists the various sensitivity test models and the corresponding outputs. It can be seen that the results of the tests span the values from our Standard Model, but are all in reasonable agreement. We feel that the results of the Standard Model are robust. We also feel that the Standard model is preferred because the parameters used were the "best" estimates of the true geometric and mechanical parameters.

9.0 CONCLUSIONS

A synthetic seismicity model of the Wellington region has been implemented. The synthetic model contains 58 known major faults and 3000 randomly placed small faults. The synthetic catalogue of 500,000 events, magnitude 5.5 or more, successfully reproduces various known features of the regional seismicity such as rate of activity, long-term slip rates, spatial distribution of hypocentres, b-value, and moment scaling. The synthetic catalogue indicates that there is a significant short-term (10 years) clustering of characteristic events throughout the region. The synthetic catalogue also gives the average recurrence time of characteristic Wellington Fault events (960 years) and their Coefficient of Variation (0.40). However, when we look at the specific effect of the 1848 Awatere and 1855 Wairarapa mega-earthquakes on the timing of the next characteristic (magnitude 7.35 or more) earthquake on the Wellington-Hutt Valley section of the Wellington Fault, we find that, on average over several hundred cases, a Wellington Fault event is delayed by 259 years. There is also a strong retarding effect on moderate magnitude Wellington Fault events, magnitude 6.5 – 7.3. From the synthetic catalogue it is possible to determine the average recurrence rate for all major faults. Regional moment release rate can be highly variable over time scales of a few hundred years.

REFERENCES

Abaimov, S., D. Turcotte, R. Shcherbakov, J. Rundle, G. Yakovlev, C. Goltz, and W. Newman (2008). Earthquakes; recurrence and interoccurrence times .*Pure and Applied Geophysics,* 165, 777-795.

Aki, K. and P. Richards (2002), Quantitative Seismology, 2nd Edition. University Science Books, Herndon, VA, USA.

Barnes, P.M., Pondard, N., Lamarche, G., Mountjoy, J., Van Dissen, R., Litchfield, N., 2008, It's Our Fault: Active faults and earthquake sources in Cook Strait. NIWA Client Report WLG2008-56: 36 p.

Barnes, P. and J. Audru (1999). Quaternary faulting in the offshore Flaxbourne and Wairarapa basins, southern Cook Strait, New Zealand. *New Zealand Journal of Geology and Geophysics*, 42, 349-367.

Barnes, P., N. Pondard, G. Lamarche,. J. Mountjoy, R. Van Dissen, N. Litchfield (2008). It's Our Fault: active faults and earthquake sources in Cook Strait. NIWA Client Report WLG2008-56

Beavan, J., Wallace, L., 2008, It's Our Fault – Wellington geodetic and GPS studies: task completion report – Fault coupling results from inversion of new and reprocessed GPS campaign data from the Wellington region. GNS Science Consultancy Report 2008/172.

Beeler, N., R. Simpson, A. Lockner, and S. Hickman (2000). Pore fluid pressure, apparent friction and Coulomb failure. *Journal of Geophysical Research,* 105, 25,533- 25,554.

Ben-Zion, Y. (1996), Stress, slip and earthquakes in models of complex single-fault systems incorporating brittle and creep deformation*, Journal of Geophysical Research, 101*, 5677-5708.

Darby, D. and S. Beanland (1992). Possible source models for the 1855 Wairarapa earthquake, New Zealand**.** *Journal of Geophysical Research*, 97, 12,375-12,389.

Dieterich, J. (1994). Earthquake simulations with time-dependent nucleation and long-range interactions. *In:* Proceedings of the 9th joint meeting of the U.J.N.R. Panel on Earthquake Prediction Technology, Anonymous. *Proceedings of the Joint Meeting of the U.J.N.R. Panel on Earthquake Prediction Technology*, 9 241-268.

Downes, G., D. Dowrick, E. Smith, and K. Berryman (1999). The 1934 Pahiatua earthquake sequence; analysis of observational and instrumental data. *Bulletin of the New Zealand National Society for Earthquake Engineering*, 32, 221-245.

Downes, G., D. Dowrick, R. Van Dissen, J. Taber, G. Hancox, and E. Smith (2006). The 1942 June 24 M_s 7.2, August 1 M_s 7.0 and December 2 M_s 6.0, Wairarapa, New Zealand, earthquakes; analysis of observational and instrumental data. Earthquake Commission, Wellington, New Zealand.

Downes, G., D. Dowrick, R. Van Dissen, J. Taber, G. Hancox, and E. Smith (2001). The 1942 Wairarapa, New Zealand, earthquakes; analysis of observational and instrumental data**.** *Bulletin of the New Zealand National Society for Earthquake Engineering*, 34, 125-157.

Fitzenz, D. and S. Miller (2001). A forward model for earthquake generation on interacting faults including tectonics, fluids, and stress transfer*, Journal of Geophysical Research, 106*, 26,689-26,706.

Grapes, R. and H. Wellman (1986). The north-east end of the Wairau Fault, Marlborough, New Zealand*. Journal of the Royal Society of New Zealand*, 16, 245-250.

Grapes, R. and G. Downes (1997). The 1855 Wairarapa, New Zealand, earthquake; analysis of historical data. Bulletin of the New Zealand Society for Earthquake Engineering, 30, 271-368.

Grapes, R., T. Little, and G. Downes (1998). Rupturing of the Awatere Fault during the 1848 October 16 Marlborough earthquake, New Zealand; historical and present day evidence (*in* Beanland memorial issue). *New Zealand Journal of Geology and Geophysics*, 41, 387-399.

Han, Z (2003). Wellington-Hutt Valley might become stable after the 1855, Wairarapa M8.2 earthquake. *Annals of Geophysics*, 46, 1141-1154.

Harris, R. (1998). Introduction to special section: Stress triggers, stress shadows, and implications for seismic hazard*, Journal of Geophysical Research, 103*, 24, 347-24,358.

Harris, R. and S. Day (1999). Dynamic 3D simulations of earthquakes on en echelon faults. *Geophysical Research Letters*, 26, 2089-2092.

Heaton, T. (1990). Evidence for and implications of self-healing pulses of slip in earthquake rupture, *Physics of the Earth & Planetary Interiors, 64*, 1-20.

King, G. and M. Cocco (2000). Fault Interaction by elastic stress changes: New clues from earthquake sequences, *Advances in Geophysics, 44*, 1-36.

Langridge, R., Van Dissen, R., Villamor, P., Little, T., 2009, It's Our Fault – Wellington Fault paleo-earthquake investigations: final report. GNS Science Consultancy Report 2008/344. 45 p.

Litchfield, N., R. Van Dissen, R. Langridge, D. Heron, and C. Prentice (2004). Timing of the most recent surface rupture event on the Ohariu Fault near Paraparaumu, New Zealand. *New Zealand Journal of Geology and Geophysics*, 47, 123-127

Little, T.A., Van Dissen, R., Rieser, U., Smith, E.G.C., Langridge, R., in review, Co-seismic strike-slip at a point during the last four earthquakes on the Wellington fault near Wellington, New Zealand. Journal of Geophysical Research (in review).

Little, T.A., Van Dissen, R., Schermer, E., Carne, R., 2009, Late Holocene surface ruptures on the southern Wairarapa fault, New Zealand: link between earthquakes and the raising of beach ridges on a rocky coast. Lithosphere 1(1): 4-28. doi:10.1130/L7.1.

Nicol, A. and J. Beavan, J. (2003). Shortening of an overriding plate and its implications for slip on a subduction thrust, central Hikurangi Margin, New Zealand. *Tectonics,* 22, 1070 doi:10.1029/2003TC001521.

Nicol, A., C. Mazengarb, F. Chanier, G. Rait, C. Uruski, and L. Wallace (2007). Tectonic evolution of the active Hikurangi subduction margin, New Zealand, since the Oligocene. *Tectonics 26,* TC4002, doi:10.1029/2006TC002090.

Okada, Y. (1992). Internal deformation due to shear and tensile faults in a half-space, *Bulletin of the Seismological Society of America, 82*, 1018-1040.

Pondard, N., P. Barnes, G. Lamarche, and J. Mountjoy (2007). Active faulting and seismic hazard in Cook Strait using high-resolution seismic data (*in* Geological Society of New Zealand and New Zealand Geophysical Society joint annual conference; launching International Year of Planet Earth, 26-29 November 2007, Tauranga; program and abstracts). *Geological Society of New Zealand Miscellaneous Publication* (2007), 123A 132

Reed, R. and R. Marks (1999). Neural Smithing: Supervised Learning in Feedforward Artificial Neural Networks. MIT Press, Cambridge.

Reyners, M. and S. Bannister (2007). Earthquakes triggered by slow slip at the plate interface in the Hikurangi subduction zone, New Zealand. *Geophysical Research Letters*, 34, L14305, doi:10.1029/2007GL030511.

Reyners, M. and D. Eberhart-Phillips (2009). Small earthquakes provide insight into plate coupling and fluid distribution in the Hikurangi subduction zone, New Zealand. *Earth ad Planetary Science Letters*, 212, 299-335,

Robinson, R, (1986). Seismicity, structure and tectonics of the Wellington region, New Zealand. *Geophysical Journal of the Royal Astronomical Society*, 87, 379-400.

Robinson, R. (2004). Potential earthquake triggering in a complex fault network: The northern South Island, New Zealand, *Geophysical Journal International,* 159*,* 734-748.

Robinson, R. and R. Benites (1996). Synthetic seismicity models for the Wellington region, New Zealand: Implications for the temporal distribution of large events, *Journal of Geophysical Research, 101*, 27,833-27,845.

Robinson, R. and R. Benites (2001). Upgrading a synthetic seismicity model for more realistic fault ruptures, *Geophysical Research Letters 28*, 1843-1846.

Robinson, R., A. Nicol, J. Walsh and P. Villamor (2009). Features of earthquake occurrence in a complex normal fault network: Results from a synthetic seismicity model of the Taupo Rift, New Zealand. In Press: *Journal of Geophysical Research*.

Rundle, P., J. Rundle, K. Tiampo., A. Donnellan and D. Turcotte (2006). Virtural California: fault model, frictional parameters, applications. *Pure and Applied Geophysics, 163,* 1819-1846.

Schermer, E., R. Van Dissen, K. Berryman, H. Kelsey and S. Cashman (2000). Active faults, paleoseismology and historical fault rupture in northern Wairarapa, North Island, New Zealand, *New Zealand. New Zealand Journal of Geology and Geophysics,* 47, 101-122.

Wallace, L., J. Beavan, R. McCaffrey and D. Darby (2004). Subduction zone coupling and tectonic block rotation in the North Island, New Zealand. *Journal of Geophysical Research, 109,* no. B12, doi: 10.1029/2004JB003241.

Wallace, L., M. Reyners, U. Cochran, S. Bannister, P. Barnes, .K. Berryman, G. Downes, D. Eberhart-Phillips, A. Nicol, R. McCaffrey, J. Beavan, S. Ellis, W. Power, S. Henrys, R. Sutherland, N. Litchfield, J. Townend, R. Robinson, D. Barker, D., and K. Wilson (2009). Characterizing the seismogenic zone of a major plate boundary subduction thrust: the Hikurangi Margin, New Zealand. *G-Cubed*. Submitted June 2009.

Ward, S. (2000). San Francisco Bay Area earthquake simulations: a step toward a standard physical earthquake model. *Bulletin of the Seismological Society of America, 90,* 370 - 386.

Webb, T. and H. Anderson (1998). Focal mechanisms of large earthquakes in the North Island of New Zealand; slip partitioning at an oblique active margin. *Geophysical Journal International*, 134, 40-86.

Webb, T., P. Somerville, D. Doser, D. Rhoades and A. Pancha (1999). Moment-Area scaling of crustal earthquakes in New Zealand. GNS Science Client Report 1999/119.

Wesnousky, S. (2008). Displacement and geometrical characteristics of earthquake surface ruptures: Issues and Implications for seismic-hazard analysis and the process of earthquake rupture*. Bulletin of the Seismological Society of America, 98*, 1609 - 1632.

Zachariasen, J., K. Berryman, R. Langridge, C. Prentice, M. Rymer, M. Stirling, P. Villamor (2006). Timing of late Holocene surface rupture of the Wairau Fault, Marlborough.. New Zealand Journal of Geology and Geophysics, 49, 159-174.

Table 1 Fault and Segment Data

I	Name	J	E1	N1	E2	N2	Strike	Dip	Rake	Slip
1	Jordan	1	-92.46	-112.99	-80.55	-89.02	206.42	40.00	110.00	20.00
2	Kekerengu	1	-80.55	-89.02	-65.24	-76.23	230.11	60.00	135.00	20.00
2	Kekerengu	2	-65.24	-76.23	-51.09	-71.77	252.53	80.00	153.00	20.00
3	Needles	1	-51.09	-71.77	-31.15	-44.11	215.79	80.00	157.00	16.00
4	Wairneedles	1	-33.15	-48.15	-17.55	-36.57	233.41	70.00	180.00	11.00
4	Wairneedles	2	-17.55	-36.57	2.11	-26.58	243.07	70.00	180.00	11.00
5	Wairarapa	1	2.83	-25.30	30.50	2.22	225.16	70.00	180.00	11.00
5	Wairarapa	2	30.50	2.22	56.35	27.10	226.09	70.00	160.00	11.30
5	Wairarapa	3	56.35	27.10	80.79	55.64	220.57	70.00	165.00	6.00
6	Booboo	1	-6.53	-48.26	-26.61	-46.60	274.73	90.00	180.00	7.00
6	Booboo	2	-6.53	-48.26	15.78	-43.54	78.06	90.00	180.00	10.00
6	Booboo	3	46.88	-43.57	15.78	-43.54	270.06	90.00	180.00	10.00
7	Wellwhv	1	-21.30	-20.58	-11.16	-14.66	239.69	70.00	-135.00	7.00
7	Wellwhv	2	-11.16	-14.66	-5.99	-6.42	212.17	80.00	155.00	7.00
7	Wellwhv	3	-5.99	-6.42	0.59	1.22	40.69	90.00	180.00	7.00
7	Wellwhv	4	0.59	1.22	23.32	17.76	53.97	75.00	-165.00	7.00
7	Wellwhv	5	23.32	17.76	36.06	23.19	66.90	65.00	-150.00	6.50
8	Wellt	1	38.26	21.65	41.38	23.05	245.81	65.00	-135.00	6.10
8	Wellt	2	41.38	23.05	57.62	42.43	219.96	70.00	180.00	6.10
8	Wellt	3	57.62	42.43	65.56	64.61	199.71	60.00	145.00	6.10
9	Alfmakuri	1	80.79	55.64	87.75	57.46	255.35	70.00	-110.00	6.00
9	Alfmakuri	2	87.75	57.46	117.13	95.73	217.52	70.00	165.00	3.50
9	Alfmakuri	3	117.13	95.73	123.60	110.13	204.19	70.00	165.00	3.50
10	Awatere	1	-124.65	-84.49	-62.71	-37.56	232.85	75.00	160.00	6.00
10	Awatere	2	-62.71	-37.56	-43.53	-26.89	240.91	80.00	180.00	1.50
11	Wellp	1	65.56	64.61	82.74	91.50	212.58	80.00	170.00	5.70
11	Wellp	2	82.74	91.50	104.89	119.11	218.74	80.00	170.00	5.70
12	Palliserkaiw	1	47.82	-39.71	100.12	-9.81	240.25	65.00	130.00	5.00
12	Palliserkaiw	2	100.12	-9.81	143.76	-4.56	263.14	75.00	160.00	4.00
13	Hopeoffsh	1	-92.46	-112.99	-54.43	-95.06	244.75	70.00	152.00	5.00
13	Hopeoffsh	2	-54.43	-95.06	-23.08	-74.80	237.13	65.00	130.00	3.50
14	Clarence	1	-115.07	-99.34	-79.26	-69.60	230.29	60.00	140.00	4.50
14	Clarence	2	-79.26	-69.60	-62.56	-60.52	241.47	70.00	140.00	4.50
15	Vernon	1	-62.71	-37.56	-60.83	-31.48	17.16	65.00	110.00	4.50
15	Vernon	2	-60.83	-31.48	-48.96	-27.19	70.13	80.00	180.00	4.50
15	Vernon	3	-48.96	-27.19	-43.53	-26.89	86.90	70.00	-115.00	2.50
15	Vernon	4	-27.13	-27.70	-43.53	-26.89	92.83	60.00	-113.00	4.50
16	Wairau	1	-125.62	-38.58	-50.12	-10.51	69.61	85.00	-175.00	4.00
16	Wairau	2	-50.12	-10.51	-34.74	-7.22	77.92	75.00	-146.00	4.00
16	Wairau	3	-23.61	-9.25	-34.74	-7.22	100.35	65.00	-125.00	4.00
17	Campbell	1	-23.79	-68.12	-16.11	-64.00	241.79	70.00	130.00	3.00
17	Campbell	2	-16.11	-64.00	-6.53	-48.26	211.33	60.00	115.00	3.00
18	Chancet	1	-51.09	-71.77	-25.31	-68.09	261.87	80.00	-174.00	3.00
19	Mascarin	1	4.48	61.12	11.13	69.31	39.09	70.00	90.00	3.00
19	Mascarin	2	11.13	69.31	31.28	116.05	23.32	70.00	90.00	3.00
20	Saunwaipukaka	1	94.04	64.66	124.52	84.72	236.65	70.00	165.00	2.50
20	Saunwaipukaka	2	124.52	84.72	130.43	95.43	208.90	70.00	165.00	2.50
21	Wharekauhau	1	-1.68	-35.02	10.69	-28.62	242.63	45.00	90.00	2.50
21	Wharekauhau	2	10.69	-28.62	30.52	-2.78	217.51	45.00	90.00	2.50
21	Wharekauhau	3	30.52	-2.78	30.78	2.03	183.06	45.00	90.00	2.50
22	Carterton	1	56.35	27.10	75.62	29.13	83.98	70.00	-135.00	2.40
22	Carterton	2	75.62	29.13	110.81	40.39	72.26	75.00	-150.00	2.40
22	Carterton	3	110.81	40.39	114.44	43.60	48.53	75.00	120.00	2.40
23	Ngapotiki	1	47.84	-38.78	51.12	-20.54	190.18	45.00	100.00	2.00
23	Ngapotiki	2	51.12	-20.54	53.29	-17.82	218.54	55.00	115.00	2.00
24	Terapa	1	-23.08	-74.80	-6.47	-73.44	265.33	80.00	160.00	2.00
24	Terapa	2	-6.47	-73.44	7.77	-67.25	246.51	70.00	130.00	2.00
25	Cloudy	1	-48.96	-27.19	-41.20	-19.89	46.76	80.00	180.00	1.50
25	Cloudy	2	-41.20	-19.89	-37.29	-19.21	80.09	70.00	-120.00	1.50

25	Cloudy	3	-27.86	-21.77	-37.29	-19.21	105.18	60.00	-110.00	1.50
26	Masterton	1	61.24	31.59	85.32	38.65	73.67	65.00	-158.00	1.50
27	Northohariu	1	31.47	53.29	37.60	56.66	61.25	90.00	180.00	1.50
27	Northohariu	2	37.60	56.66	44.57	65.00	39.90	90.00	180.00	1.50
27	Northohariu	3	44.57	65.00	59.46	73.11	61.40	90.00	180.00	1.50
27	Northohariu	4	59.46	73.11	72.76	88.84	40.23	90.00	180.00	1.50
28	Ohariuc	1	6.37	17.39	11.38	22.28	45.66	90.00	180.00	1.50
28	Ohariuc	2	11.38	22.28	29.11	49.09	33.48	75.00	155.00	1.50
29	Oharius	1	-29.62	-18.78	-17.98	-13.98	247.60	65.00	-130.00	1.50
29	Oharius	2	-17.98	-13.98	-12.18	-9.27	230.94	70.00	-154.00	1.50
29	Oharius	3	-12.18	-9.27	6.37	17.39	214.83	75.00	160.00	1.50
30	Opouawe	1	49.15	-51.97	111.88	-32.45	252.72	60.00	150.00	1.50
30	Opouawe	2	111.88	-32.45	169.00	0.51	240.01	60.00	110.00	1.50
31	Pahaua	1	45.32	-60.57	114.08	-40.87	254.01	60.00	150.00	1.50
31	Pahaua	2	114.08	-40.87	153.89	-16.46	238.49	60.00	110.00	1.50
32	Fisherman	1	-15.42	19.85	-7.98	35.27	205.75	75.00	100.00	1.00
32	Fisherman	2	-7.98	35.27	17.25	65.47	219.87	75.00	100.00	1.00
32	Fisherman	3	17.25	65.47	25.96	86.01	202.98	75.00	100.00	0.70
33	Kaumingi	1	82.86	22.80	107.33	29.03	255.71	70.00	-150.00	1.00
34	KekerenguBF	1	-54.84	-126.53	-9.41	-83.01	226.23	55.00	130.00	1.00
35	Whareama	1	108.65	-5.29	128.72	15.66	223.77	60.00	120.00	1.00
36	Onepoto	1	8.43	48.08	15.45	54.41	228.01	70.00	90.00	1.00
36	Onepoto	2	15.45	54.41	38.08	109.78	202.23	70.00	90.00	1.00
37	Upperslope	1	-47.75	-109.96	-37.85	-91.59	208.34	45.00	120.00	1.00
37	Upperslope	2	-37.85	-91.59	-21.08	-78.91	232.90	55.00	130.00	1.00
38	Rangitikeioffsh	1	27.57	78.75	35.52	97.99	22.46	70.00	90.00	1.00
38	Rangitikeioffsh	2	35.52	97.99	48.75	116.72	35.24	70.00	90.00	0.40
39	Otakiforks	1	30.47	29.44	39.39	43.84	211.77	75.00	150.00	0.80
39	Otakiforks	2	39.39	43.84	57.81	64.64	41.53	90.00	180.00	0.80
40	Okupe	1	-16.15	2.47	6.34	49.42	205.60	75.00	100.00	0.80
40	Okupe	2	6.34	49.42	12.99	57.61	219.07	75.00	100.00	0.80
41	Dryhuang	1	25.93	-31.37	58.85	1.66	224.91	65.00	90.00	0.70
41	Dryhuang	2	58.85	1.66	66.94	5.87	242.49	65.00	90.00	0.70
41	Dryhuang	3	66.94	5.87	70.08	12.44	205.47	65.00	90.00	0.70
42	Manaota	1	-12.61	-2.23	-1.42	19.59	207.15	75.00	100.00	0.20
42	Manaota	2	-1.42	19.59	8.77	31.04	221.65	75.00	100.00	0.30
42	Manaota	3	8.77	31.04	31.33	76.99	206.16	65.00	100.00	0.60
43	Akatarawa	1	23.32	17.76	30.47	29.44	211.45	75.00	150.00	0.60
44	Mokonuine	1	87.86	47.82	111.47	55.19	72.68	70.00	-158.00	0.50
45	Mokonuisw	1	65.45	36.47	87.86	47.82	63.13	90.00	180.00	0.50
46	Pukeshep	1	-12.61	-2.23	-7.90	2.68	43.75	90.00	180.00	0.50
46	Pukeshep	2	-7.90	2.68	-4.29	9.09	29.44	90.00	180.00	0.50
46	Pukeshep	3	-4.29	9.09	11.67	29.31	38.28	90.00	180.00	0.50
47	Shannona	1	53.01	74.59	63.91	85.76	224.29	60.00	90.00	0.20
48	Moonshine	1	2.12	7.67	30.47	29.44	52.48	90.00	180.00	0.20
49	Otaraia	1	29.71	-24.43	45.32	-2.97	216.03	60.00	90.00	0.20
49	Otaraia	2	45.32	-2.97	49.75	0.98	228.27	60.00	90.00	0.20
50	Poroutawhao	1	36.02	60.96	44.43	81.29	202.48	60.00	90.00	0.20
51	Bidwill	1	48.59	4.53	59.13	11.47	236.67	60.00	90.00	0.20
51	Bidwill	2	59.13	11.47	60.31	13.65	208.38	60.00	90.00	0.20
52	Himatangiant	1	45.53	85.71	57.05	108.91	206.40	60.00	90.00	0.20
53	Levinant	1	42.78	72.08	52.37	82.38	222.95	60.00	90.00	0.20
54	Martinborough	1	51.04	2.24	62.19	10.82	232.42	65.00	90.00	0.10
54	Martinborough	2	62.19	10.82	65.23	19.25	199.84	65.00	90.00	0.10
55	Whitemans	1	10.12	-9.90	22.68	14.44	207.30	60.00	110.00	0.10
56	Subduction NE	1	45.00	-40.00	151.00	66.00	225.00	5.00	90.00	31.80
56	Subduction NE	2	-4.00	9.00	102.00	115.00	225.00	25.00	90.00	31.80
57	Subduction SW	1	-25.50	-105.50	41.50	-38.50	225.00	5.00	90.00	31.80

I = Fault Number; J = Segment Number; E1 and N1 = coordinates of one end of the segment, km; E2 and N2 = the other end; Strike, Dip and Rake are in degrees and follow the Aki & Richards (2002) convention; Slip is in mm/yr. The coordinate centre is at -41.2861, 174.7683.

Table 2 Mechanical Properties of the Standard Model.

P-Wave Velocity	6500.0 m/s
Density	2850.0 kg/m^3
Stress Propagation velocity	3000.0 m/s
$\square_{33}$ decay time[1]	10 yr
Time Step in event	0.8 s
Healing Time	3.0 s
Scale Factor[2]	0.4
Radiation Damping[3]	0.75
Coefficient of Friction	0.70 – 0.80
Skempton's Coefficient	0.5
Pore Pressure Decay Time	10 yr

[1] If the normal stress becomes too low or too high it decays with this exponential time constant.
[2] Stress factor to put all results to the equivalent of cells 1 km square.
[3] Factor to account for energy lost as elastic waves.

Table 3 Emergent Fault Properties

N	Name	Mchar	dT	CV	U1	U2
1	Jordan	7.13	633.2	0.14	-3.40	10.73
2	Kekerengu	7.21	282.8	0.57	-6.30	3.78
3	Needles	7.05	581.6	0.18	-8.04	3.48
4	Wairneedles	7.14	589.4	0.34	-7.42	-0.59
5	Wairarapa	7.65	1046.7	0.69	-7.93	2.77
6	Booboo	7.30	1407.9	0.20	-11.49	0.04
7	Wellwhv	7.35	955.9	0.41	-7.11	-2.29
8	Wellt	7.28	901.6	0.56	-7.24	-0.08
9	Alfmakuri	7.32	1961.2	0.55	-5.20	2.49
10	Awatere	7.73	3002.1	0.22	-12.42	4.51
11	Wellp	7.30	800.6	0.45	-6.39	2.22
12	Palliserkaiw	7.50	1443.6	0.51	-3.83	7.38
13	Hope Offsh	7.39	1703.0	0.48	-5.97	7.22
14	Clarence	7.15	2500.0	0.80	-4.84	2.53
15	Vernon	7.03	3055.4	0.10	-2.56	-6.52
16	Wairau	7.56	3759.8	0.16	-11.8	-2.11
17	Campbell	7.00	2460.5	0.64	-2.81	5.87
18	Chancet	6.97	1991.7	0.39	-5.34	-0.70
19	Mascarin	7.37	4335.0	0.51	1.55	8.40
20	Saunwaipukaka	7.03	2388.5	0.47	-3.97	2.78
21	Wharekauhau	6.80	2150.0	0.45	4.88	2.44
22	Carterton	7.26	2650.7	0.46	-4.60	-3.88
23	Ngapotiki	7.08	Big	0.63	0.04	4.85
24	Terapa	7.09	4126.3	0.51	-4.06	5.02
25	Cloudy	0.00	903.2	0.98	-0.26	-2.01
26	Masterton	6.71	5198.5	0.21	-5.90	-0.10
27	North Ohariu	7.24	2904.8	0.61	-3.19	-4.96
28	Ohariu Cen	7.14	3786.9	0.51	-3.72	-4.35
29	Ohariu South	7.19	49734.7	0.91	1.69	-4.52
30	Opouawe	7.61	13381.9	0.75	-4.61	7.42
31	Pahaua	7.53	8446.6	0.95	-4.51	7.67
32	Fisherman	7.30	12433.8	0.59	5.85	0.12
33	Kaumingi	6.83	5738.0	0.43	-3.80	3.45
34	KekerenguBF	7.32	24043.0	0.59	5.96	0.19
35	Whareama	7.21	5176.0	0.12	-2.07	12.15
36	Onepoto	7.12	27407.8	0.59	-0.43	6.95
37	Upper Slope	7.06	6089.2	0.63	-0.95	-6.66
38	Rangitikei offsh	7.23	39234.6	0.75	4.45	-3.61

39	Otakiforks	7.25	25883.9	0.98	-5.59	-1.41
40	Okupe	7.18	5598.5	0.49	5.26	-1.94
41	Dryhuang	7.30	3044.0	0.53	5.10	3.42
42	Manaota	7.46	41076.7	0.49	7.14	-2.47
43	Akatarawa	6.60	4041.6	0.56	-1.02	-4.13
44	Mokonuine	6.96	5764.4	0.66	-3.21	-3.68
45	Mokonuisw	6.87	8283.5	0.55	-2.58	-4.03
46	Pukeshep	6.84	2753.7	0.52	0.73	-4.60
47	Shannona	6.77	4050.8	0.42	1.70	-4.51
48	Moonshine	7.00	3073.6	0.32	6.23	1.15
49	Otaraia	7.03	4290.4	0.52	4.25	-2.10
50	Poroutawhao	6.88	4597.3	0.30	-0.29	-5.33
51	Bidwill	6.75	3168.0	0.63	3.93	-1.46
52	Himatangi Ant	6.97	9653.8	0.42	1.15	-6.75
53	Levin Ant	6.41	6568.9	0.28	2.32	-3.50
54	Martinborough	6.65	36914.7	0.42	3.49	-1.50
55	Whitemans	6.80	1847.6	0.29	5.18	-4.37
56	Subduction NE	7.80	See Text	0.72	-0.81	6.71
57	Subduction SW	7.40	See text	0.75	2.01	2.47

Mchar= Characteristic magnitude, dT = Average recurrence time for characteristic events; CV = Coefficient of variation for dT; U1 = Strike-slip in characteristic events, meters (negative is right-lateral); U2 = Dip-slip in characteristic events, meters (negative is down-dip (normal faulting), positive is up-dip (thrusting).

Table 4 Results of Sensitivity Tests.

Name	Average dT, yrs	COV	Bias, yrs
Standard	962	0.40	259
Vertical W. Fault	973	0.16	156
West Dip W/ Fault	950	0.40	270
Lower Friction	987	0.25	143
No Subduction.	833	0.27	89
Lower Pore Pres.	922	0.33	219
Asperity	930	0.31	216
No Healing	1224	0.30	199
No Small Faults	933	0.32	224
Visco-elastic	913	0.29	119
Bigger Stress Drop	1101	0.45	265
DEF = 1.0	982	0.50	265
DEF = 2.0	899	0.45	210
Diff. Init. Condits.	973	0.38	215
“	981	0.43	248
“	955	0.43	260
“	959	0.39	264

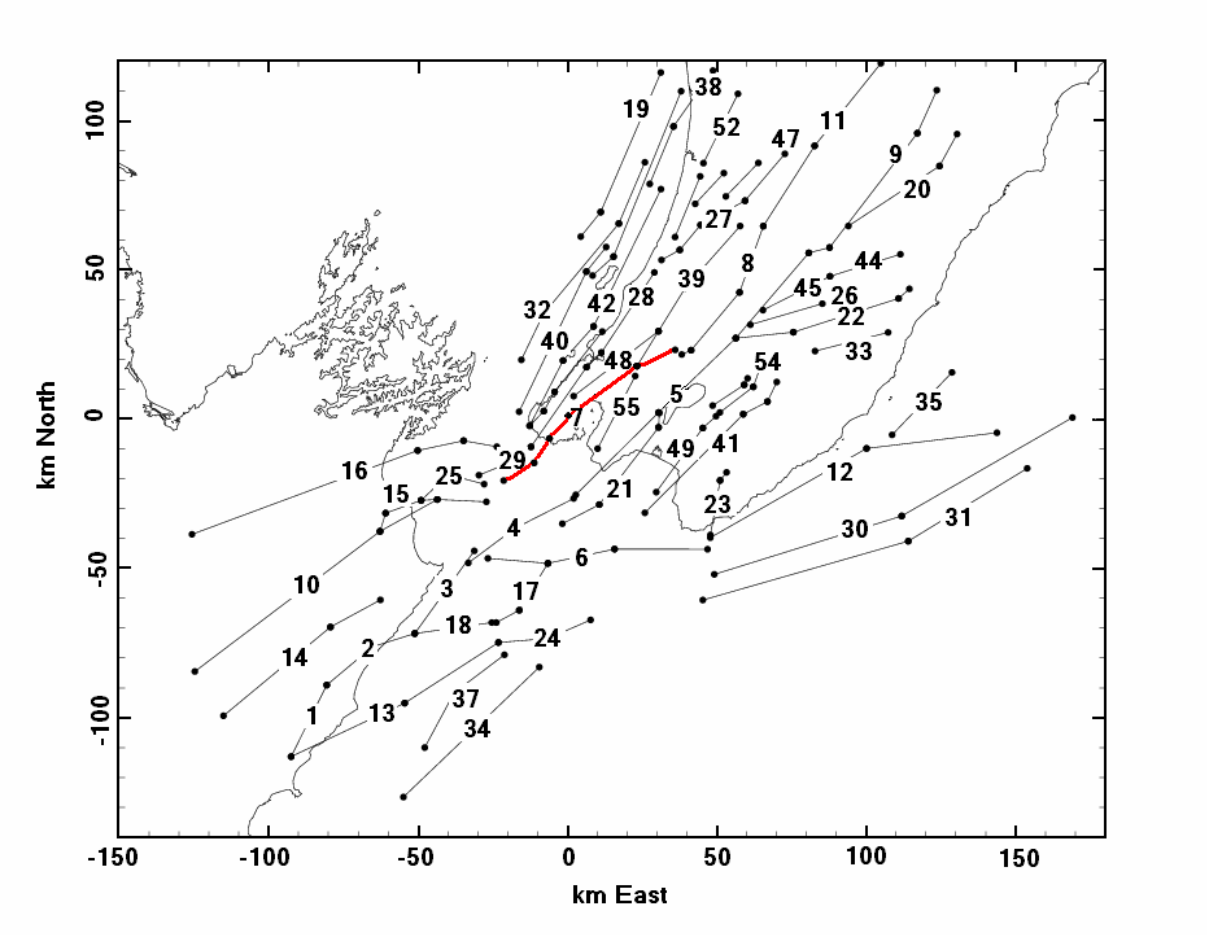

Figure 1 Map of the Wellington Region and the major faults above the plate interface. The numbers correspond to those in Table 1 except that a few are left out due to over-crowding. The Wellington-Hutt Valley section of the Wellington Fault is highlighted in red. The coordinate system is taken from the New Zealand Map Grid with the centre redefined as the position of the WEL seismograph station at Kelburn.

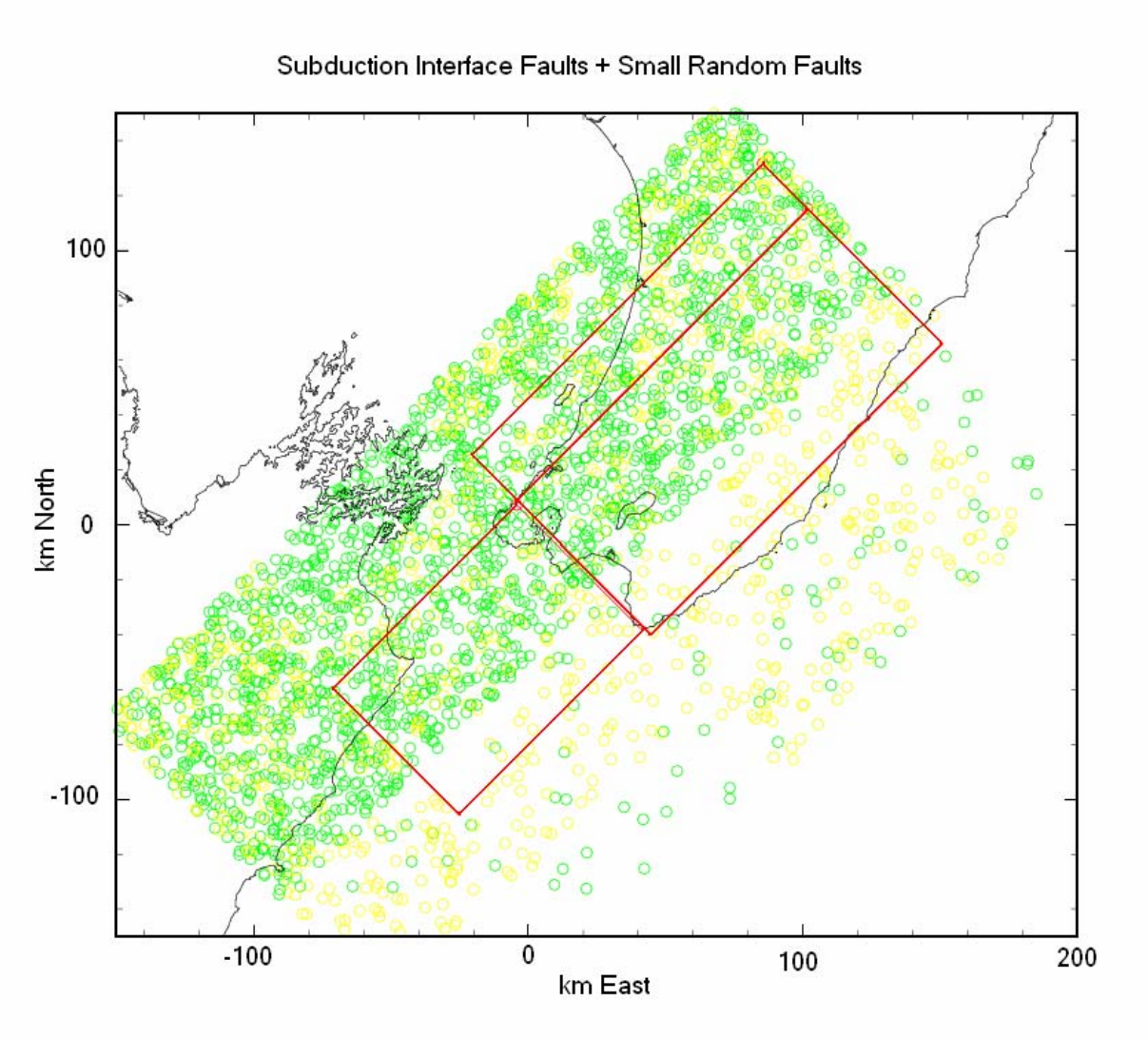

Figure 2 Map of the Wellington Region showing the surface projections of the section of the plate interface on which seismic slip is allowed (red). The yellow circles represent the 1000 small, random faults above the plate interface. The green circles represent the 2000 small, random faults below the plate interface.

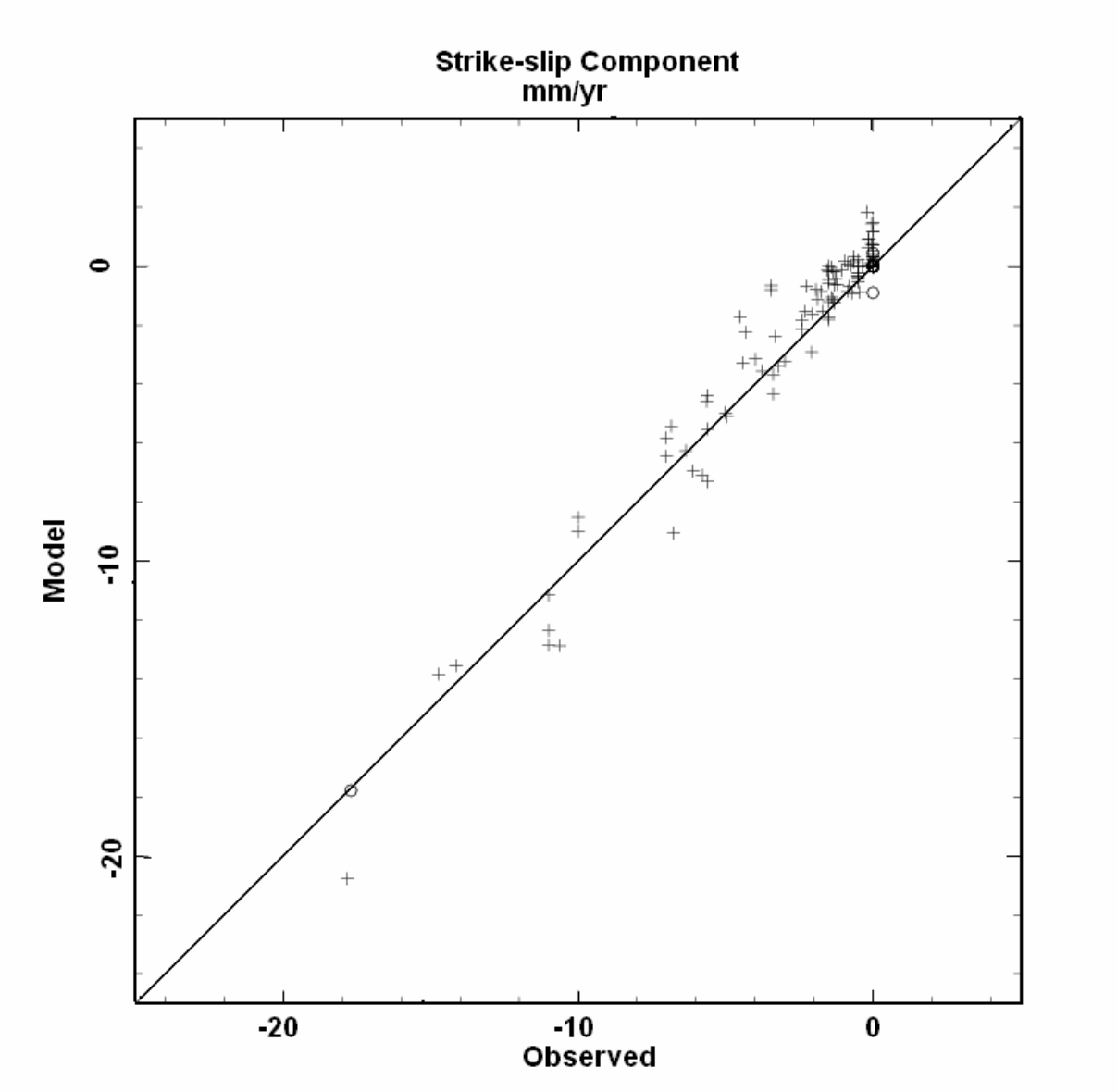

Figure 3a Comparisons of the long-term slip rates for the synthetic model and those observed geologically (in mm/year). **A**: for the strike-slip component (negative if right-lateral). **B**: For the dip-slip component (negative is for normal faulting, positive for thrust). Circles are for the subduction interface.

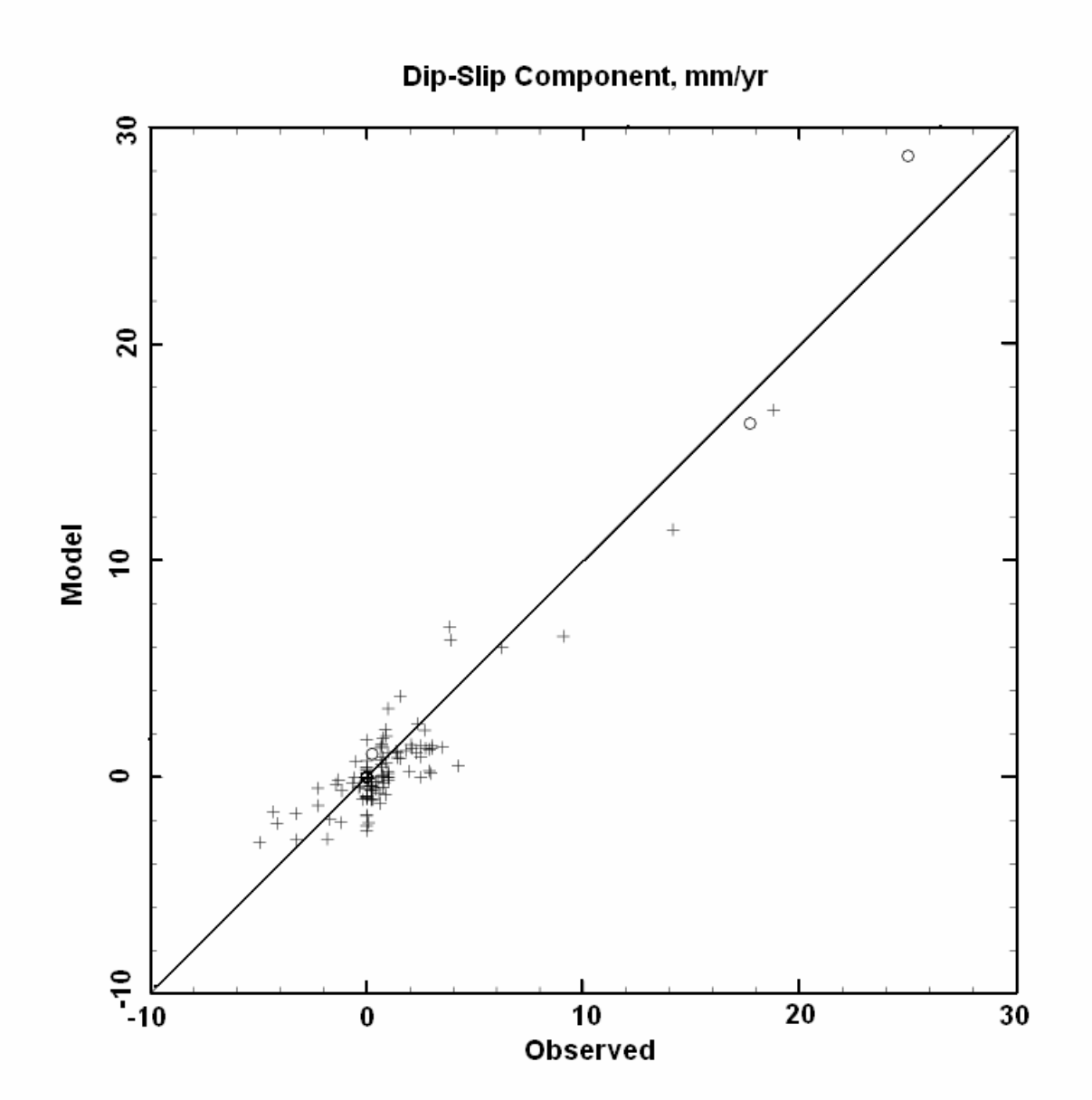

Figure 3b Comparisons of the long-term slip rates for the synthetic model and those observed geologically (in mm/year). **A**: for the strike-slip component (negative if right-lateral). **B**: For the dip-slip component (negative is for normal faulting, positive for thrust). Circles are for the subduction interface.

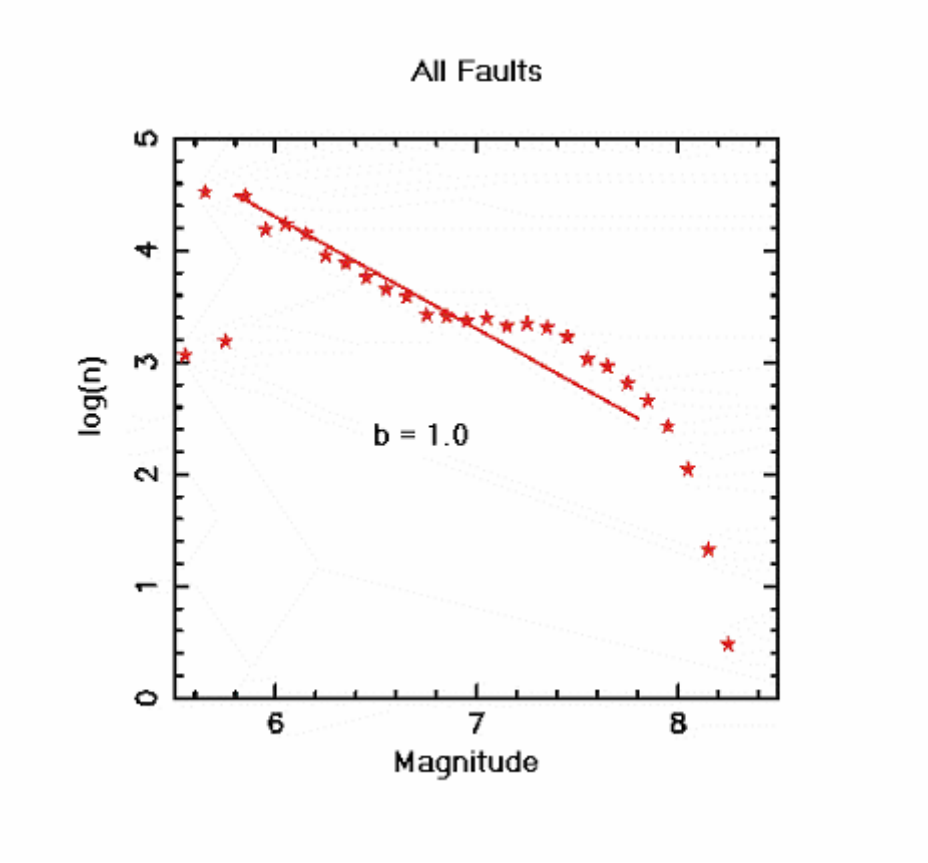

Figure 4 Frequency – Magnitude plot for the region as a whole. Note that the numbers are not cumulative.

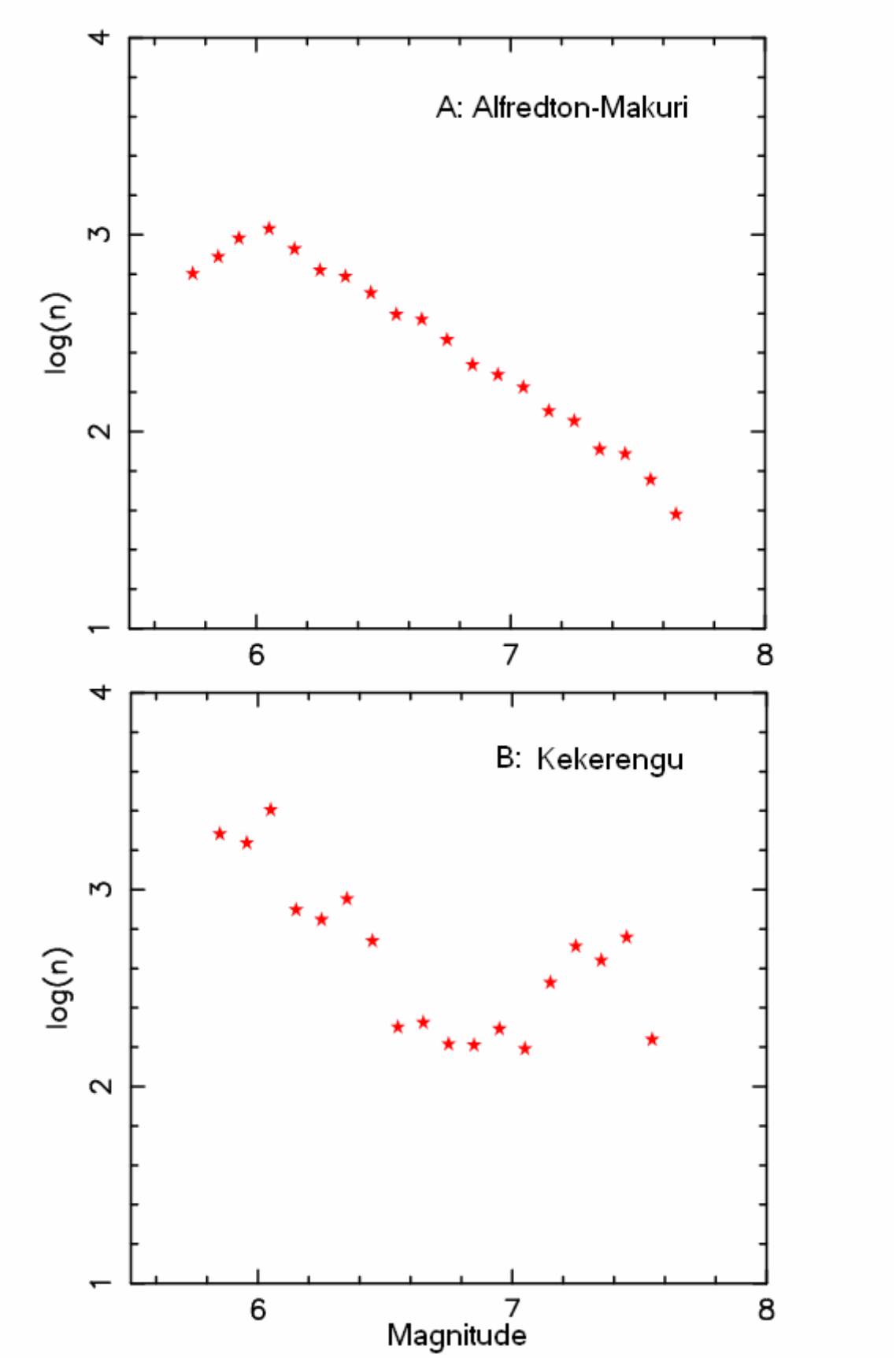

Figure 5 Frequency – Magnitude plots for two individual faults that show extreme types of behaviour. **A**: Gutenberg-Richter behaviour for the Alfredton-Makuri Fault. **B**: Characteristic behaviour for the Kekerengu Fault.

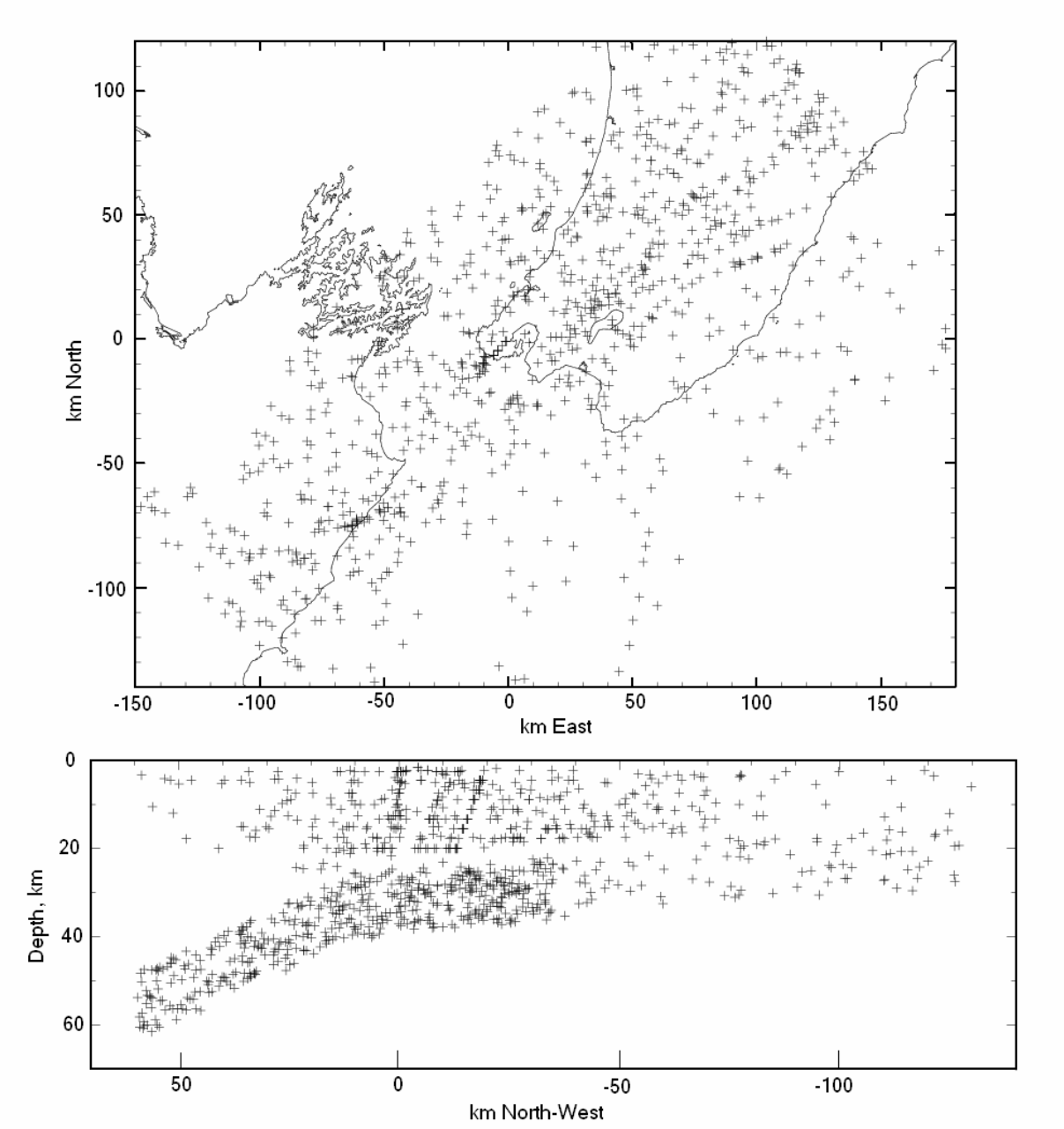

Figure 6 Example of the spatial distribution of hypocentres in the synthetic catalogue for the time period 55,000 -56,000 years. **Top**: Map view of all epicentres. **Bottom**: NorthWest – SouthEast cross-section.

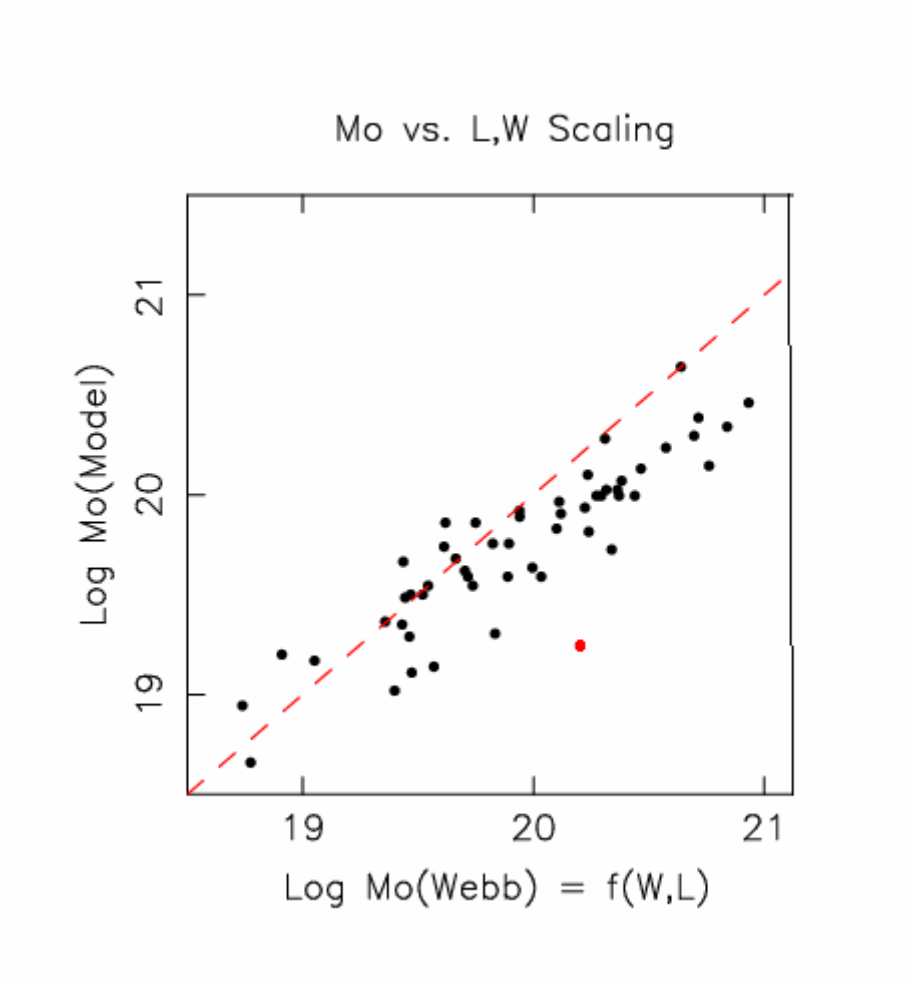

Figure 7 Moment scaling for characteristic events. Horizontal axis = log10(Moment) expected from the scaling relations of Webb et al. (1999). Vertical axis = Moment of characteristic events form the synthetic seimicity model. Red dot = Whaekaukau Fault. Red dashed line shows a ration of 1:1.

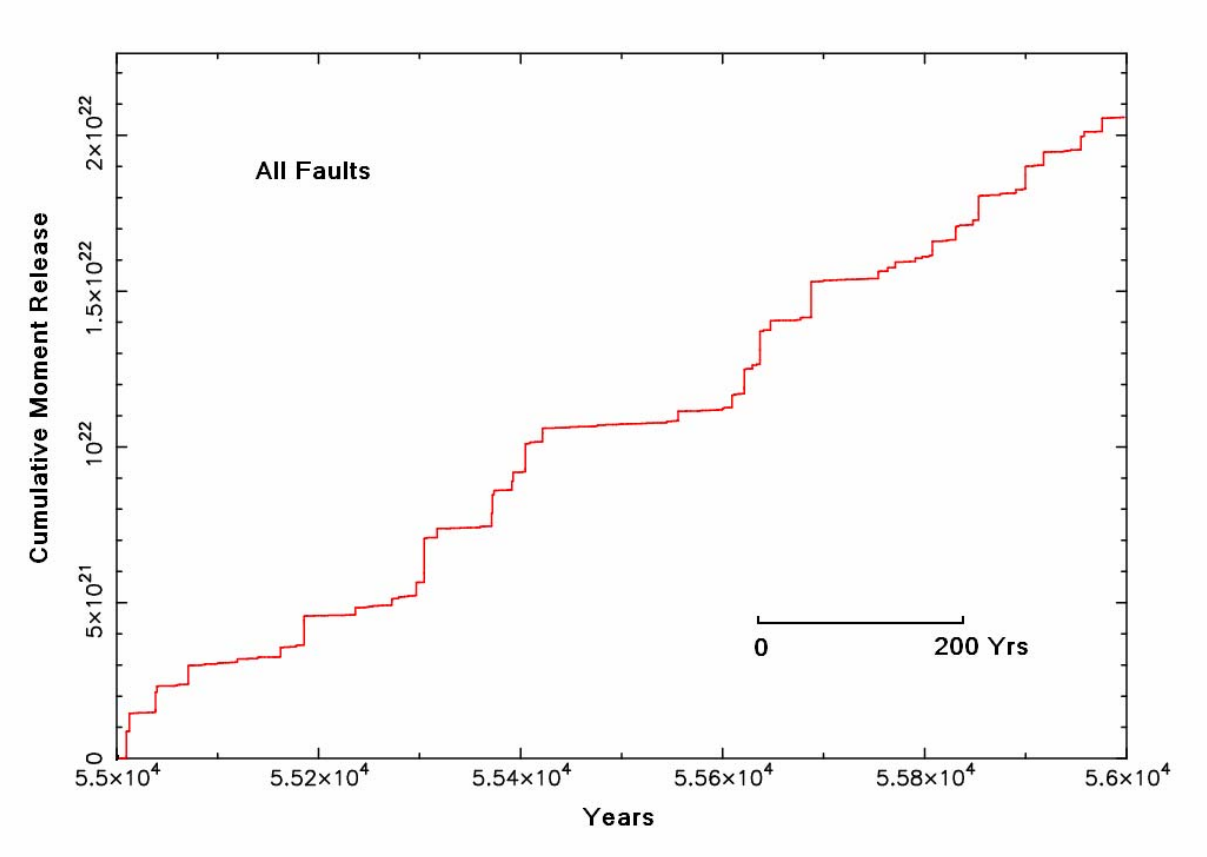

Figure 8 Cumulative moment release vs. time for the period 55,000 – 56,000 years. Note the considerable variations over time spans of 100 – 200 years which would make extrapolating the actual historic record very dangerous.

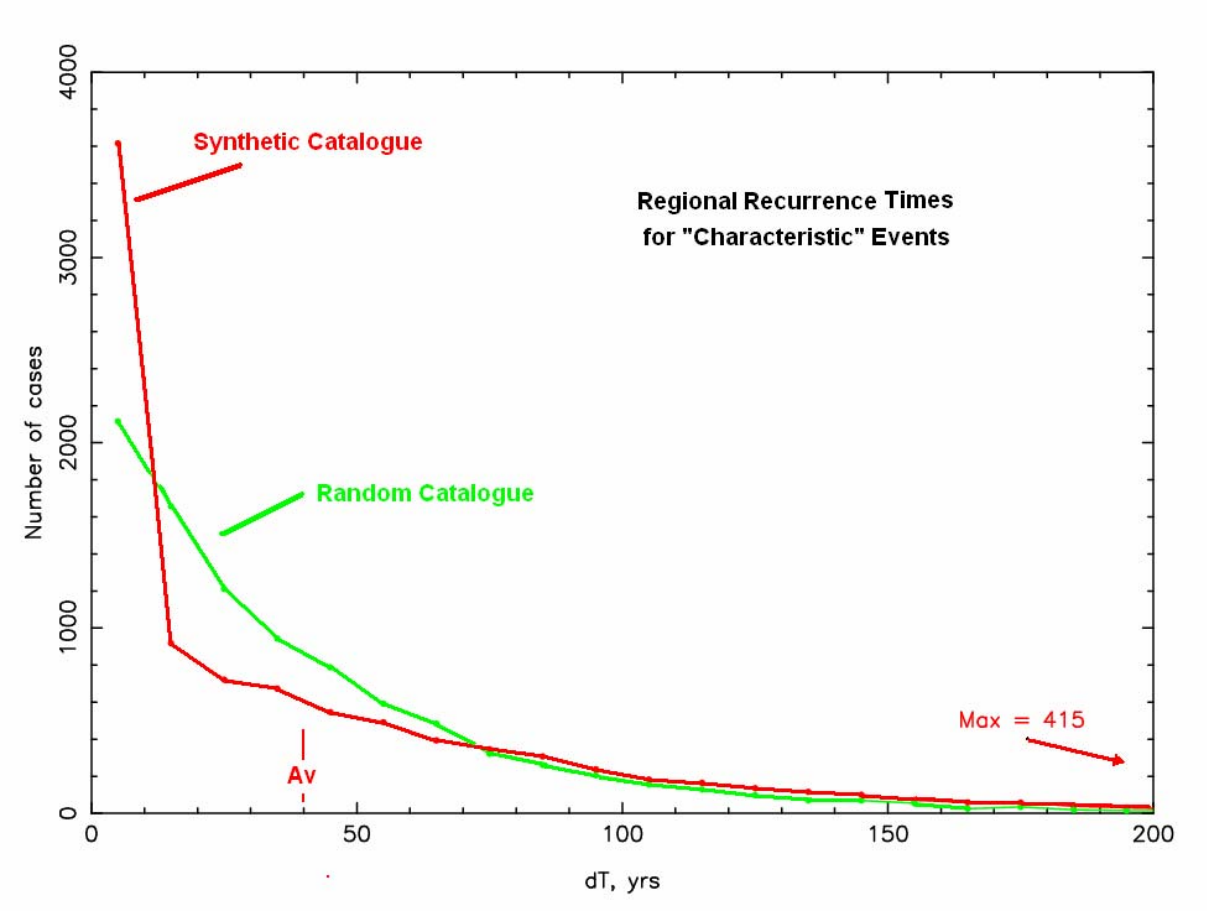

Figure 9 Distribution of recurrence time for characteristic events on any fault. The red curve is for the synthetic catalogue, the green for a randomized catalogue. Events in the synthetic catalogue show considerable short-term temporal clustering followed by relative quiescence.

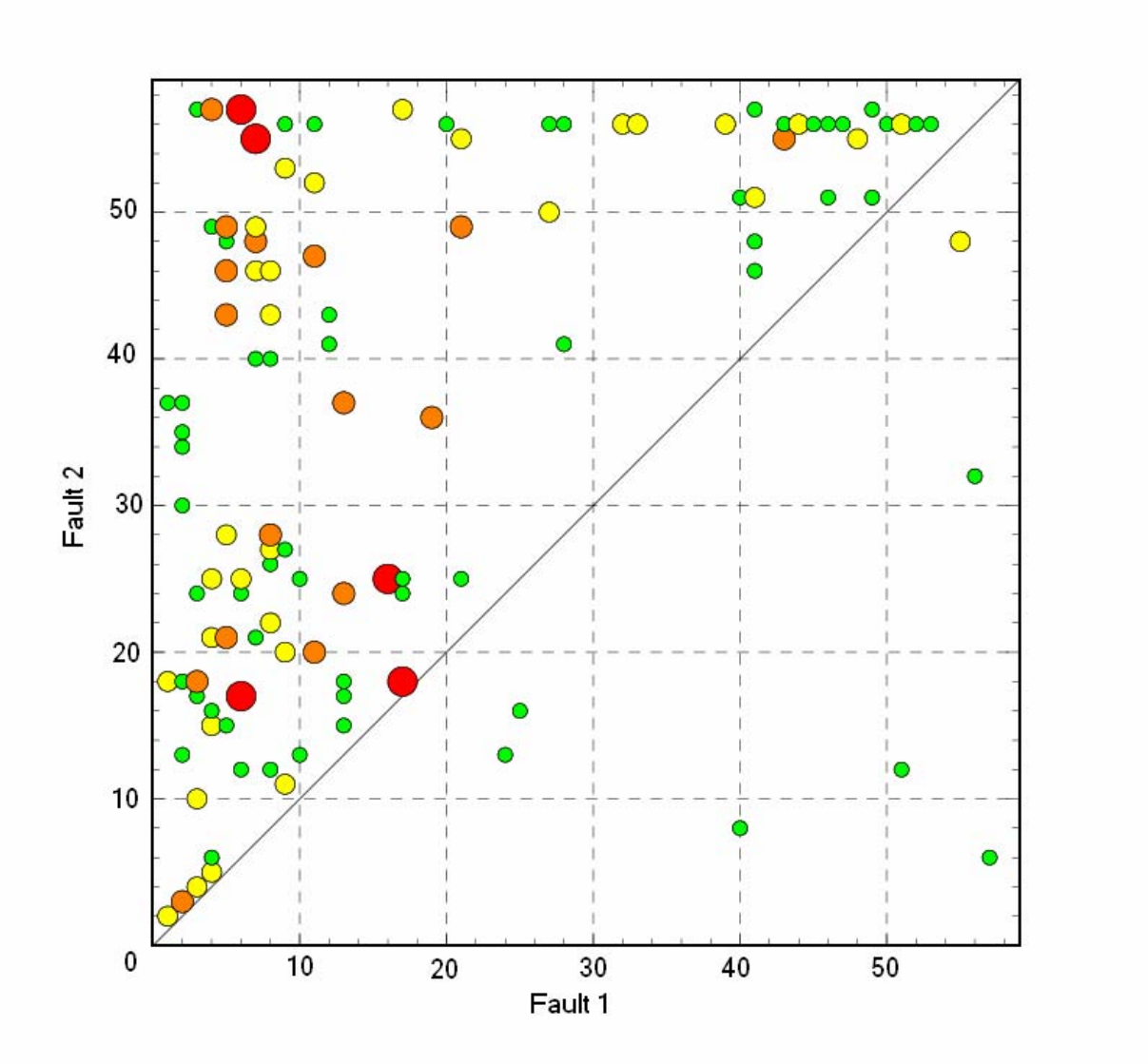

Figure 10 Interaction matrix for characteristic events. A circle is plotted if the number of events on Fault 2, within 10 years following a n event on Fault 1, is significantly larger than expected by chance. Large red circles = bigger by a factor of 15 or more; orange circles = bigger by a factor of 10 - 15; yellow circles = bigger by a factor of 5 - 10; green if bigger by a factor of 2.5 – 5.0. Numbers on the axes refer to the fault number as in Table 1 and Figure 1. Note that the Wellington – Hutt Valley Fault (7) is not often triggered by any other fault.

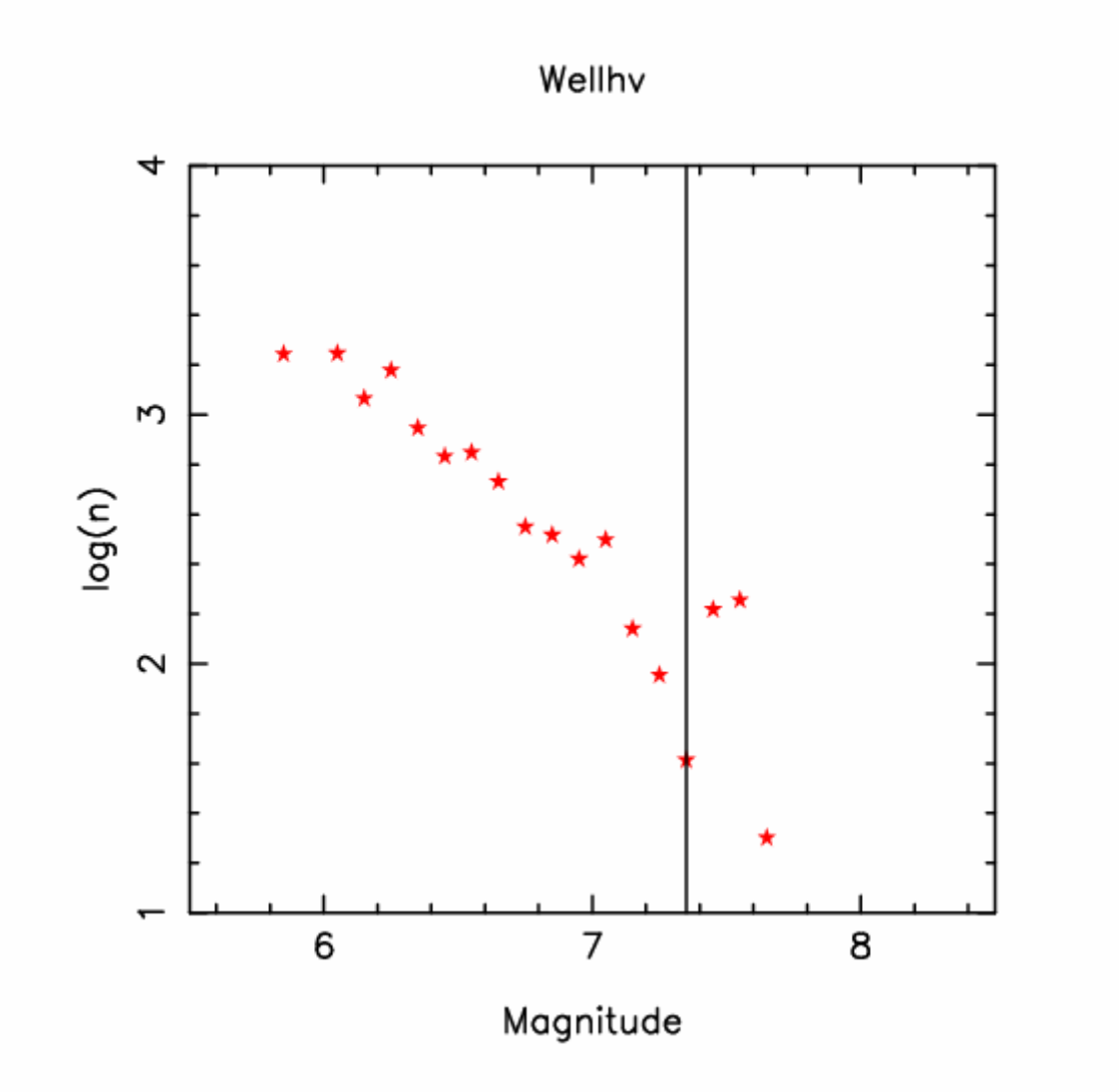

Figure 11 Frequency – Magnitude plot for the Wellington-Hutt Valley section of the Wellington Fault. The vertical black line shows the definition of M_{char}.

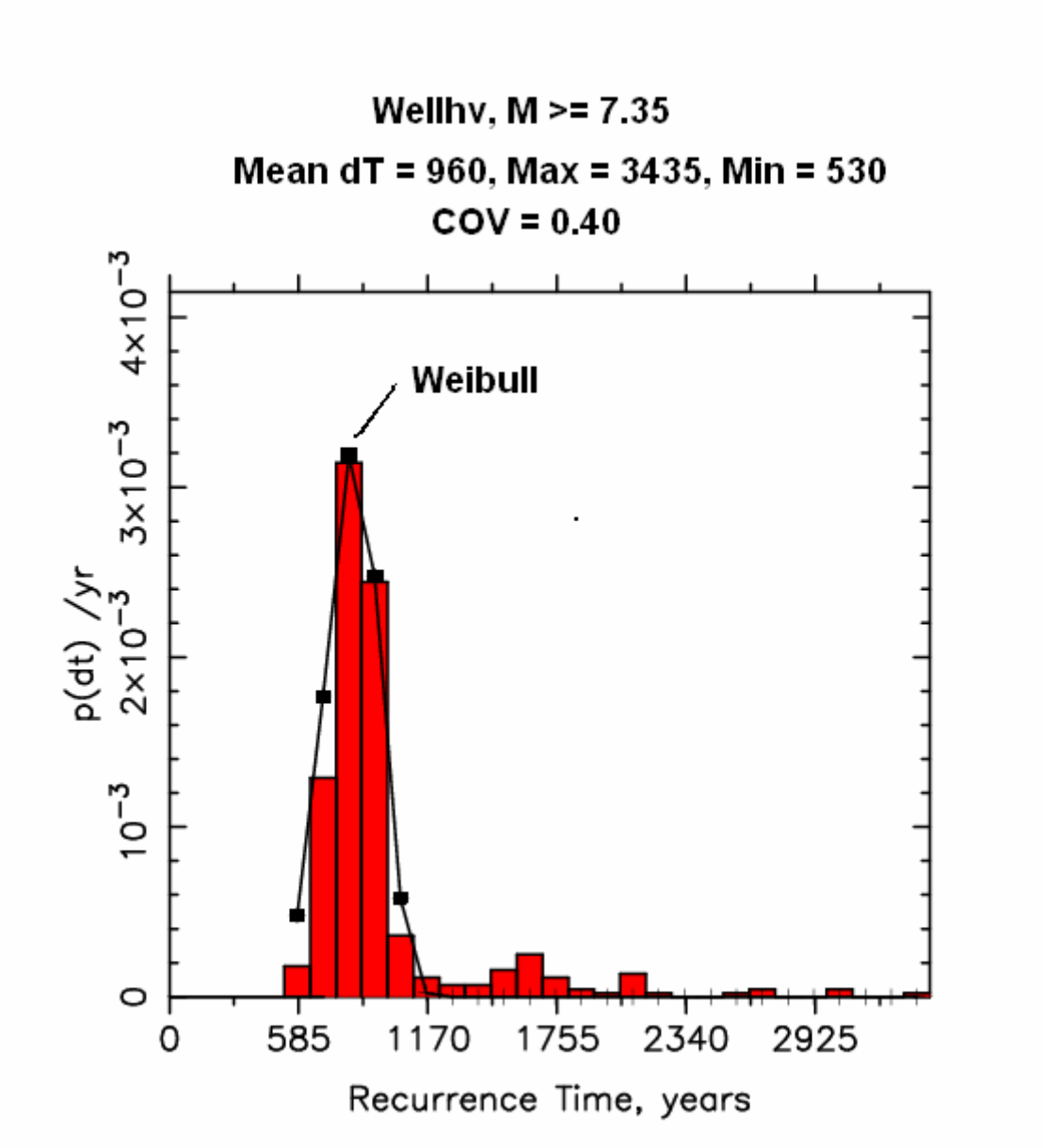

Figure 12 Histogram of recurrence time for characteristic events on the Wellington-Hutt Valley section of the Wellington Fault. The black line and symbols shows the best fitting 3-parameter Weibull distribution.

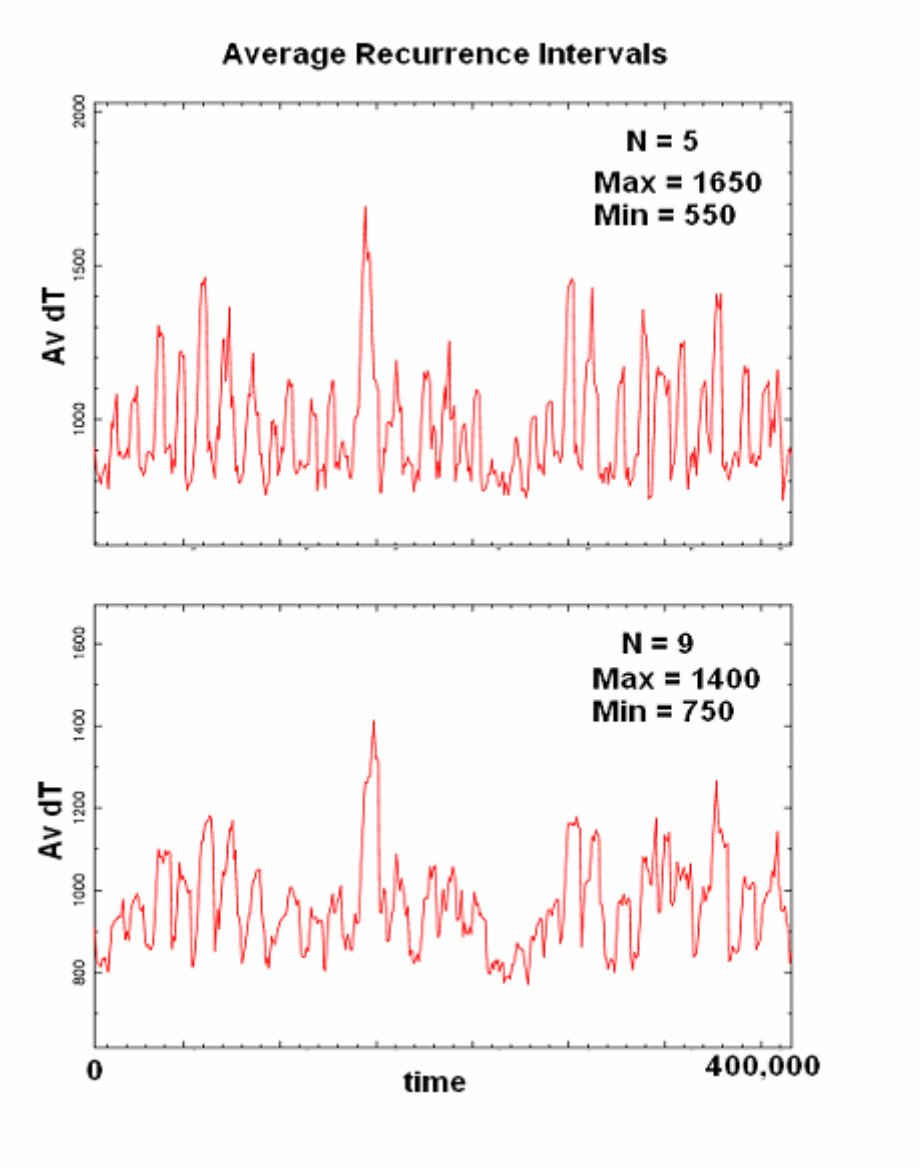

Figure 13 Moving average recurrence time vs. time for the characteristic events on the Wellington-Hutt Valley section of the Wellington Fault. Top: Averaged over four instances (5 events). Bottom: Averaged over 10 instances (9 events). Note that the vertical scales are different.

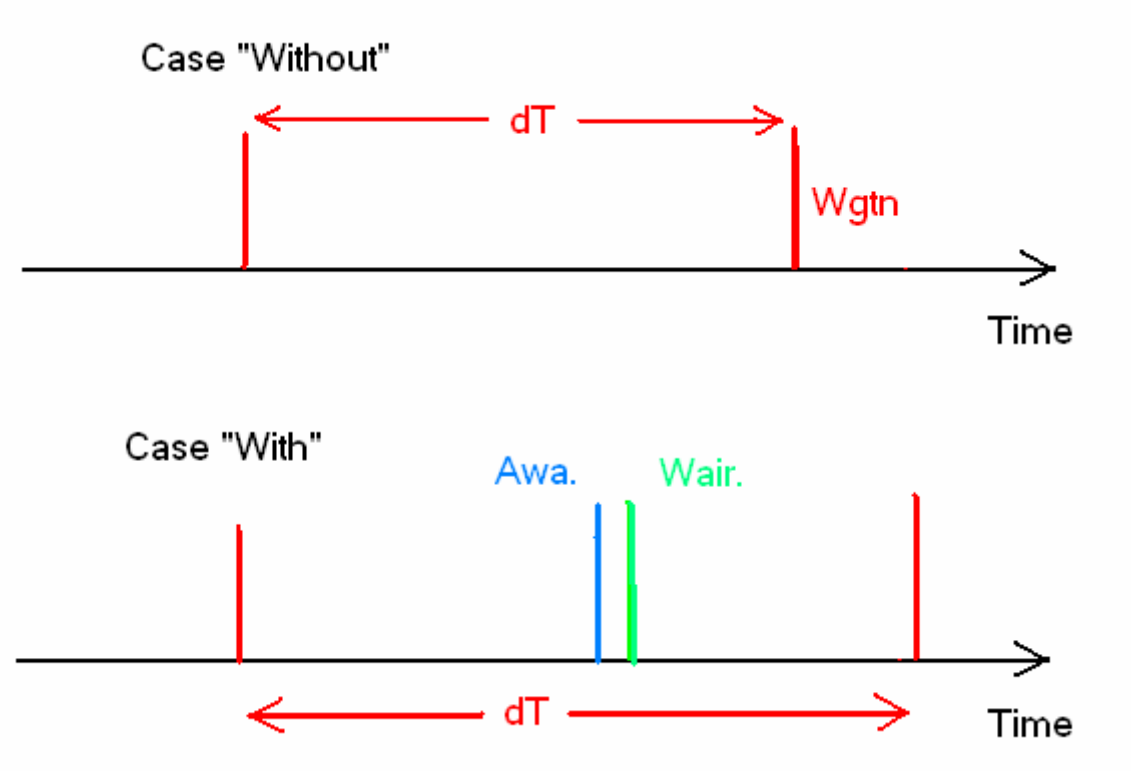

Figure 14 Cartoon showing how the two classes of recurrence time on the Wellington-Hutt Valley section of the Wellington Fault are different.

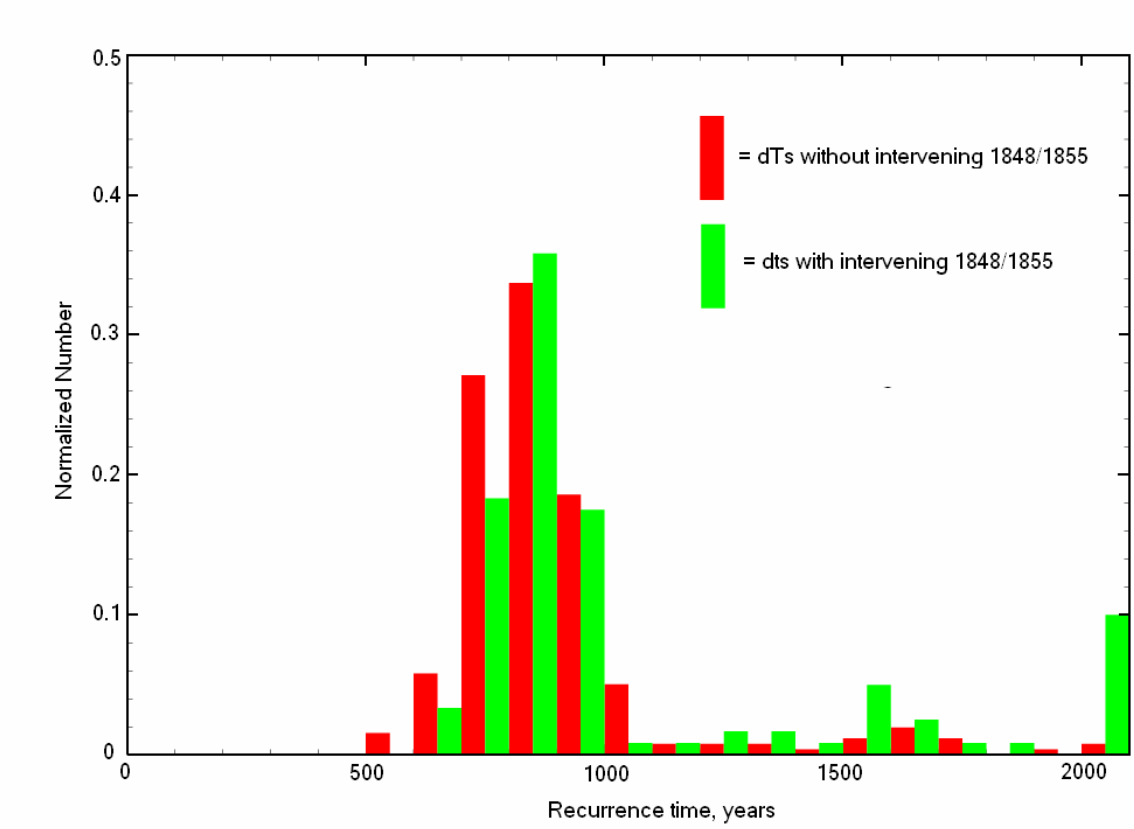

Figure 15 Normalized histograms for the two classes of recurrence times for characteristic events (M 7.35 or more) on the Wellington-Hutt Valley section of the Wellington Fault. Note that for each 100 year bin there are two bars, one red, and one green, for the same bin but displaced for clarity.

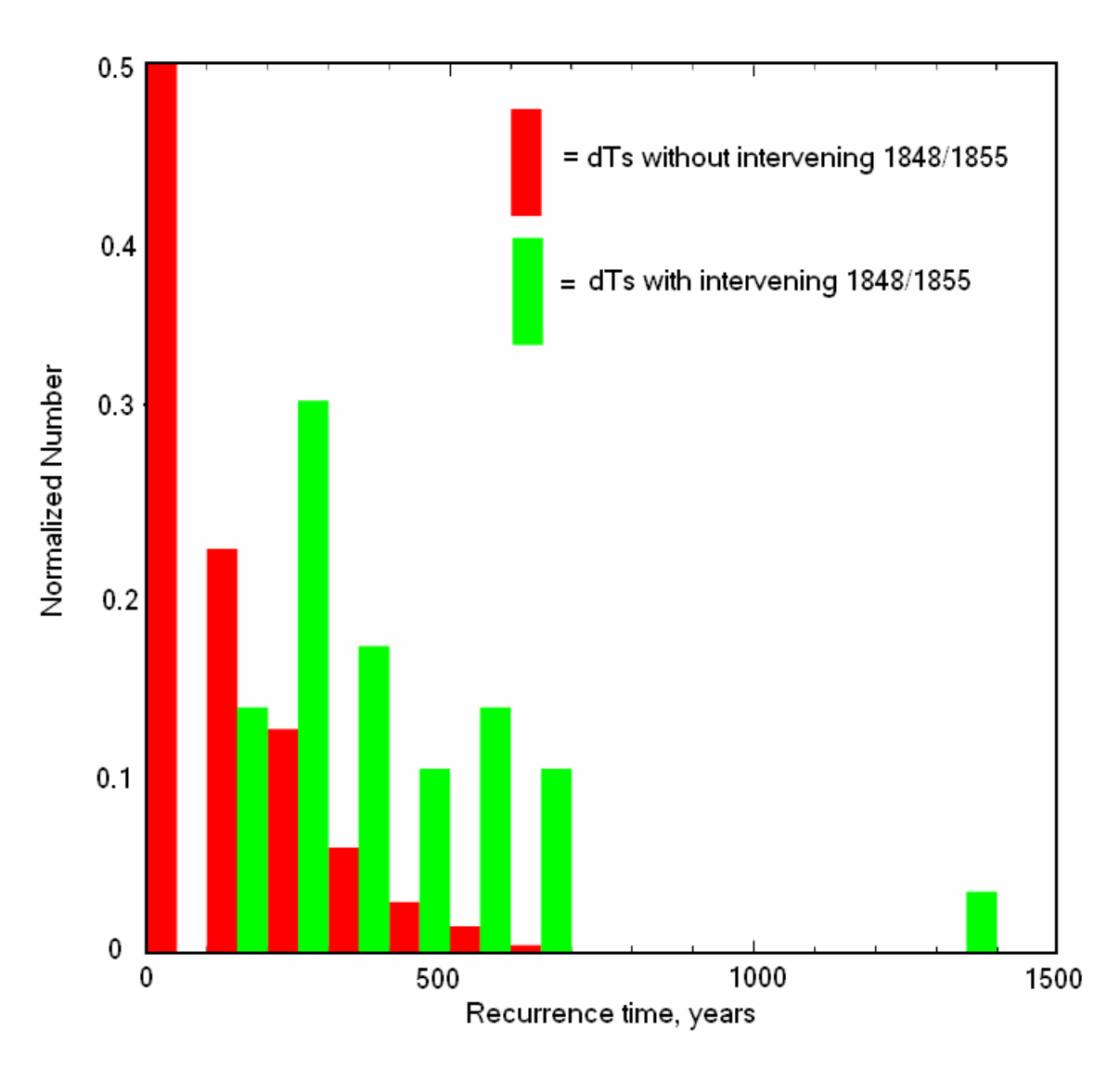

Figure 16 Normalized histograms for the two classes of recurrence times for moderate events (M 6.5 – 7.3) on the Wellington-Hutt Valley section of the Wellington Fault.

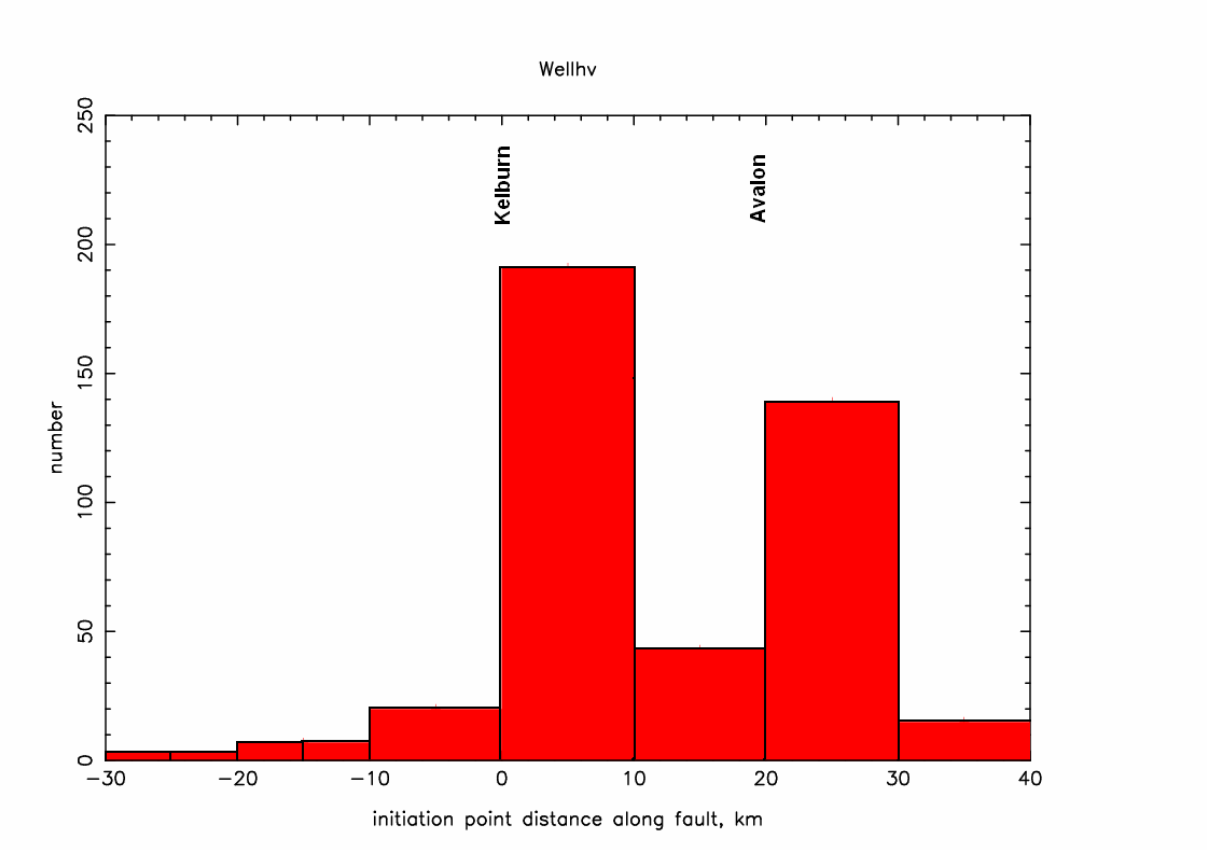

Figure 17 Histogram for the positions of epicentres of characteristic events on the Wellington-Hutt Valley section of the Wellington Fault. The horizontal axis is the distance along the fault measured from the south end.

www.gns.cri.nz

Principal Location

1 Fairway Drive
Avalon
PO Box 30368
Lower Hutt
New Zealand
T +64-4-570 1444
F +64-4-570 4600

Other Locations

Dunedin Research Centre
764 Cumberland Street
Private Bag 1930
Dunedin
New Zealand
T +64-3-477 4050
F +64-3-477 5232

Wairakei Research Centre
114 Karetoto Road
Wairakei
Private Bag 2000, Taupo
New Zealand
T +64-7-374 8211
F +64-7-374 8199

National Isotope Centre
30 Gracefield Road
PO Box 31312
Lower Hutt
New Zealand
T +64-4-570 1444
F +64-4-570 4657